

WM RECORD COPY

NNWS1 1663  
#19

GEOHYDROLOGY OF TEST WELL USW H-3, YUCCA MOUNTAIN,  
NYE COUNTY, NEVADA

WM DOCKET CONTROL  
CENTER

~~'85 APR -2 A10:41~~

U.S. GEOLOGICAL SURVEY

Water-Resources Investigations Report 84-4272

Prepared in cooperation with the  
U.S. DEPARTMENT OF ENERGY



GEOHYDROLOGY OF TEST WELL USW H-3, YUCCA MOUNTAIN,  
NYE COUNTY, NEVADA

By William Thordarson<sup>1</sup>, F. E. Rush<sup>1</sup>, and S. J. Waddell<sup>2</sup>

---

U.S. GEOLOGICAL SURVEY

Water-Resources Investigations Report 84-4272

Prepared in cooperation with the  
U.S. DEPARTMENT OF ENERGY

<sup>1</sup>U.S. Geological Survey, Denver, Colorado

<sup>2</sup>Fenix & Scisson, Inc., Mercury, Nevada

Lakewood, Colorado

1985



UNITED STATES DEPARTMENT OF THE INTERIOR

WILLIAM P. CLARK, Secretary

GEOLOGICAL SURVEY

Dallas L. Peck, Director

---

For additional information  
write to:

Chief, Nuclear Hydrology Program  
Water Resources Division  
U.S. Geological Survey  
Box 25046, Mail Stop 416  
Denver Federal Center  
Lakewood, CO 80225

Copies of this report can be  
purchased from:

Open-File Services Section  
Western Distribution Branch  
U.S. Geological Survey  
Box 25425, Federal Center  
Lakewood, CO 80225  
Telephone: (303) 236-7476

## CONTENTS

	Page
Abstract-----	1
Introduction-----	1
Purpose and scope-----	2
Location of the well-----	2
Drilling procedures and well construction-----	2
Geohydrologic setting-----	2
Lithology-----	4
Geophysical log interpretations-----	6
Borehole-flow survey-----	9
Water-level monitoring-----	9
Hydraulic testing-----	11
Pumping tests-----	14
Injection tests-----	17
Swabbing tests-----	31
Comparison of testing and borehole-flow survey results-----	31
Discussion of well-site geohydrology-----	35
Conclusions-----	36
References cited-----	37

## ILLUSTRATIONS

	Page
Figure 1. Map showing location of test well USW H-3-----	3
2. Chart showing distribution of porous rock in the well, as determined from geophysical logs-----	7
3-20. Graphs showing:	
3. Borehole-flow survey for test well USW H-3-----	10
4. Analysis of water-level recovery following second cycle of pumping of the interval from 754 to 1,219 meters, using the straight-line method-----	15
5. Analysis of the pumping test of the interval from 754 to 1,219 meters, using Brown's method for a cyclically pumped well-----	15
6. Analysis of water-level drawdown of the interval from 822 to 1,219 meters, using the Theis method-----	16
7. Wellbore-storage effects during injection tests of the intervals from 792 to 850, 851 to 917, 1,063 to 1,124, and 1,126 to 1,219 meters-----	20
8. Wellbore-storage effects during injection tests of the intervals from 911 to 972 and 972 to 1,219 meters-----	21
9. Relation of pressure and injection rate during injection tests-----	22
10. Velocity of water in tubing during injection tests of the intervals from 792 to 850, 851 to 917, 1,063 to 1,124, and 1,126 to 1,219 meters-----	23

ILLUSTRATIONS--Continued

	Page
Figures 3-20. Graphs showing--Continued:	
11. Velocity of water in tubing during injection tests of the intervals from 911 to 972 and 972 to 1,219 meters-----	24
12. Relation of specific capacity and time during injection tests-----	25
13. Analysis of injection test of the interval from 792 to 850 meters, using the slug-test method-----	26
14. Analysis of injection test of the interval from 851 to 917 meters, using the straight-line method-----	26
15. Analysis of injection test of the interval from 911 to 972 meters, using straight-line and slug-test methods-----	27
16. Analysis of injection test of the interval from 972 to 1,219 meters, using straight-line and slug-test methods-----	28
17. Analysis of injection test of the interval from 1,063 to 1,124 meters, using straight-line and slug-test methods-----	29
18. Analysis of injection test of the interval from 1,126 to 1,219 meters, using the straight-line method-----	30
19. Analysis of recovery of water level during swabbing test of the interval from 792 to 1,219 meters-----	31
20. Analysis of recovery of water level during swabbing test of the interval from 1,063 to 1,124 meters-----	32

TABLES

	Page
Table 1. Generalized lithologic log for test well USW H-3-----	5
2. Summary of test results-----	13
3. Distribution of apparent transmissivity and hydraulic conductivity based on the borehole-flow survey-----	33
4. Comparison of transmissivity values resulting from three types of tests-----	34

## METRIC CONVERSION TABLE

For those readers who prefer to use inch-pound rather than metric units, conversion factors for the terms used in this report are listed below:

<i>Metric unit</i>	<i>Multiply by</i>	<i>To obtain inch-pound unit</i>
millimeter (mm)	$3.937 \times 10^{-2}$	inch
centimeter (cm)	$3.937 \times 10^{-1}$	inch
kilometer (km)	$6.214 \times 10^{-1}$	mile
meter (m)	3.281	foot
degree Celsius ( $^{\circ}\text{C}$ )	$1.8(^{\circ}\text{C}) + 32$	degree Fahrenheit
millimeter per year (mm/a)	$3.281 \times 10^{-3}$	foot per year
meter per minute	$4.724 \times 10^3$	foot per day
meter per day (m/d)	3.281	foot per day
meter squared per day ( $\text{m}^2/\text{d}$ )	$1.076 \times 10^1$	foot squared per day
cubic meter ( $\text{m}^3$ )	$3.531 \times 10^1$	cubic foot
liter per second (L/s)	$1.585 \times 10^1$	gallon per minute
liter per second per meter	4.831	gallon per minute per foot
degree Celsius per kilometer ( $^{\circ}\text{C}/\text{km}$ )	2.900	degree Fahrenheit per mile
kilopascal (kPa)	$1.450 \times 10^{-1}$	pound per square inch
kilopascal per meter (kPa/m)	$4.420 \times 10^{-2}$	pound per square inch per foot

---

SYMBOLS LIST

<u>Symbol</u>	<u>Description</u>	<u>Dimension</u>
b	Saturated thickness.	Meters.
H	Hydraulic head at time t after injection or removal of "slug."	Meters.
H <sub>0</sub>	Hydraulic head inside well at instant of removal of "slug."	Meters.
K	T/b; hydraulic conductivity.	Meters per day.
Q	Flow rate.	Liters per second.
r <sub>c</sub>	Radius of tubing in interval within which water level fluctuates.	Centimeters.
r <sub>s</sub>	Radius of open hole.	Centimeters.
S	Storage coefficient.	Dimensionless.
s	Drawdown.	Meters.
s'	Residual drawdown.	Meters.
T	Transmissivity.	Meters squared per day.
t	Time after pumping started.	Minutes, seconds.
t'	Time after pumping stopped.	Minutes.
t/t'	Ratio of the time after pumping started to the time after pumping stopped.	Dimensionless.
W(μ)	4π Ts/Q; W (well) function of μ.	Dimensionless.
μ	r <sup>2</sup> S/4Tt.	Dimensionless.
Δp	Pressure change.	Meters of water.
Δs	Drawdown for one log cycle.	Meters.
Δs'	Residual drawdown for one log cycle.	Meters.
α	r <sub>s</sub> <sup>2</sup> S/r <sub>c</sub> <sup>2</sup> .	Dimensionless.

GEOHYDROLOGY OF TEST WELL USW H-3, YUCCA MOUNTAIN  
NYE COUNTY, NEVADA

By William Thordarson, F. E. Rush, and S. J. Waddell

ABSTRACT

Test well USW H-3 is one of several test wells drilled in the southwestern part of the Nevada Test Site in cooperation with the U.S. Department of Energy for investigations related to the isolation of high-level radioactive wastes. All rocks penetrated by the well to a total depth of 1,219 meters are volcanic tuff of Tertiary age.

The composite hydraulic head in the zone 751 to 1,219 meters was 733 meters above sea level, and at a depth below land surface of 751 meters. Below a depth of 1,190 meters, the hydraulic head was 754 meters above sea level or higher, suggesting an upward component of ground-water flow at the site.

The most transmissive part of the saturated zone is in the upper part of the Tram Member of the Crater Flat Tuff in the depth interval from 809 to 841 meters, with an apparent transmissivity of about  $7 \times 10^{-1}$  meter squared per day. The remainder of the penetrated rocks in the saturated zone, 841 to 1,219 meters, has an apparent transmissivity of about  $4 \times 10^{-1}$  meter squared per day. The most transmissive part of the lower depth interval is in the bedded tuff and Lithic Ridge Tuff, in the depth interval from 1,108 to 1,120 meters. The apparent hydraulic conductivity of the rocks in the lower depth interval from 841 to 1,219 meters commonly ranges from about  $10^{-1}$  to  $10^{-4}$  meter per day.

INTRODUCTION

The U.S. Geological Survey has been conducting investigations at Yucca Mountain, Nevada, to evaluate the hydrologic and geologic suitability of this site for storing high-level nuclear waste in a geologic mined repository. These investigations are part of the Nevada Nuclear Waste Storage Investigations project conducted in cooperation with the U.S. Department of Energy, Nevada Operations Office, under Interagency Agreement DE-AI08-78ET44802. Test drilling has been a principal method of investigation. This report presents hydrologic information on test well USW H-3, one of several exploratory wells drilled into tuff in or near the southwestern part of the Nevada Test Site. The data used for the interpretations in this report are contained in a report by Thordarson and others (1984).

## Purpose and Scope

The primary purpose of this study is to define hydrologic characteristics of tuff in the southwestern part of the Nevada Test Site that may be useful in determining the suitability of tuffs for isolating toxic nuclear wastes. This report presents detailed hydraulic-testing data, supporting geological and geophysical information, and hydrological interpretations for the rocks penetrated in drilling the well, one of a series of test wells designed to obtain data principally for the saturated zone.

## Location of the Well

Test well USW H-3 is approximately 140 km northwest of Las Vegas in southern Nevada (fig. 1). The well site is on the main north-south oriented ridge of Yucca Mountain, northwest of Jackass Flats and 2 km west of the Nevada Test Site boundary. The well is approximately 4 km south-southwest of test well USW H-1, at Nevada State Central Zone Coordinates N 756,542 and E 558,452. Altitude of the land surface at the well site is 1,483.4 m above sea level. Test well USW H-1 was the first well in the series to be drilled; this well (USW H-3) was the second.

## Drilling Procedures and Well Construction

Drilling of the well started on January 21, 1982; total depth of 1,219 m was reached on February 28, 1982. The rotary-drilling fluid was air foam consisting of air, detergent, and water obtained from supply well J-13 (fig. 1). About 1,200 m<sup>3</sup> of detergent and water were used (Thordarson and others, 1984). Drilling was completed without much difficulty; however, circulation was lost between a depth of 392 and 817 m, and caving occurred between depths of 38 and 308 m. The well did not deviate more than 2.75 degrees from the vertical; the bottom of the well is 25 m west-northwest of the starting point at land surface. Additional well-construction details are presented by Thordarson and others (1984). In July 1982, after injection and swabbing tests were completed, but before the pumping test, the well casing was perforated below the static water level, from a depth of 754 m to the bottom of the casing at 792 m; vertical spacing of perforations is about 15 cm.

## Geohydrologic Setting

The rocks exposed in the vicinity of the Nevada Test Site consist principally of various sedimentary rocks of Precambrian and Paleozoic age, volcanic and sedimentary rocks of Tertiary age, and alluvial and playa deposits of Quaternary age (Winograd and Thordarson, 1975; Byers and others, 1976). The rocks of Precambrian and Paleozoic age have a total thickness of approximately 11,000 m; they are predominantly limestone and dolomite, but include marble, quartzite, argillite, shale, and conglomerate. The rocks of Paleozoic age have been intruded by granitic stocks of Mesozoic and Tertiary age, and by basalt dikes of Tertiary and Quaternary age. The bulk of the rocks of Tertiary age consist of welded, vitric, and zeolitic tuffs and rhyolite flows

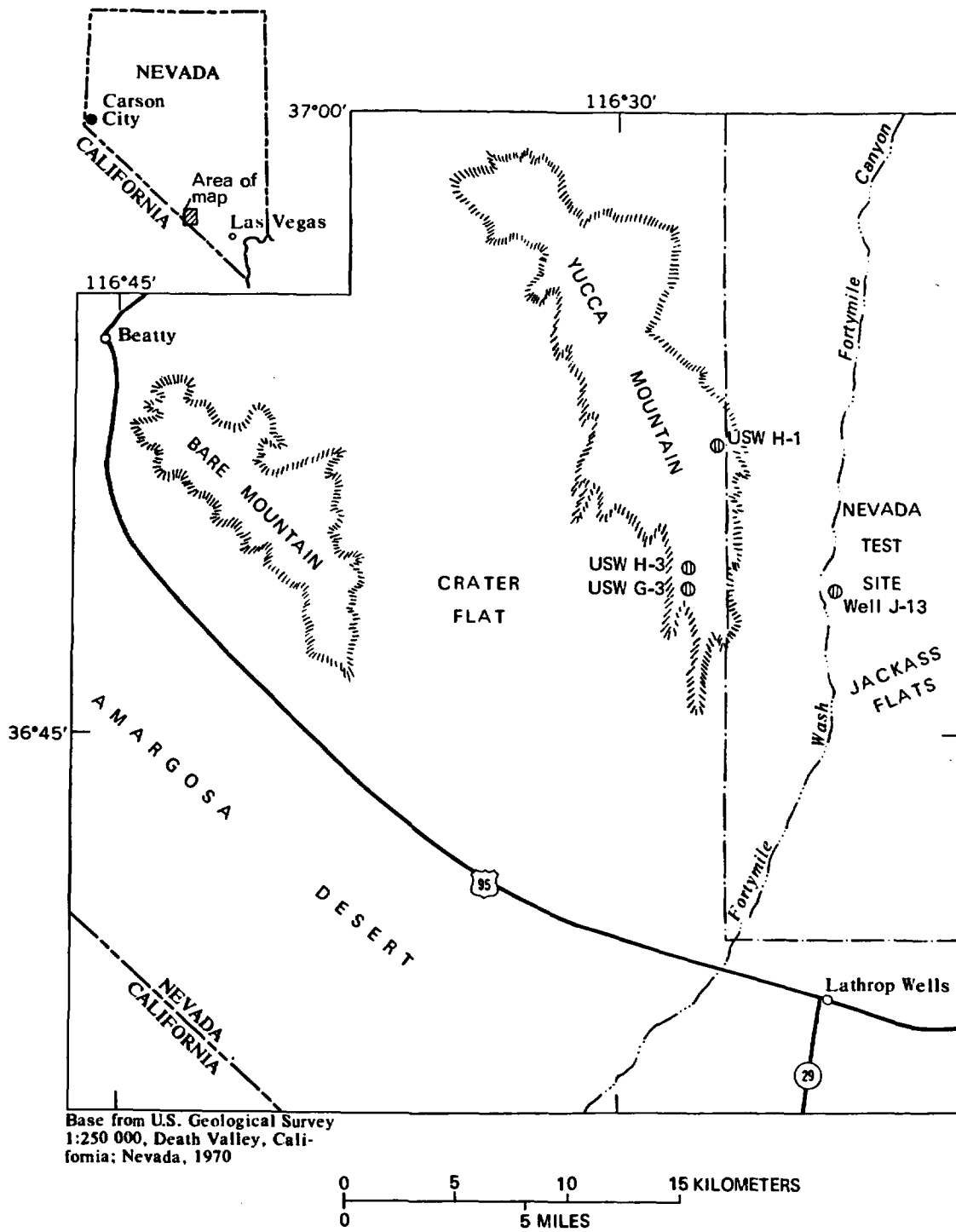


Figure 1.--Location of test well USW H-3.

of Miocene age that were extruded from the Timber Mountain-Oasis Valley caldera complex, 20 km north of the test well. The alluvium consists principally of detritus deposited in the intermontane basins, much of it as fan deposits.

Tuffs underlie Yucca Mountain from land surface to some undetermined depth in excess of 1,219 m. The pre-Tertiary lithology is unknown, but it is most likely either granite or sedimentary rocks of Paleozoic age.

Surface drainage is indirectly toward the Amargosa Desert (fig. 1). Jackass Flats (fig. 1), at an altitude of about 1,000 m above sea level, receives an average annual precipitation of about 100 mm (Hunt and others, 1966, p. B5-B7). The mountain receives more precipitation because of its higher altitude; winter and spring are the seasons with the greatest precipitation, when frontal storms move across the area from the west. During the summer, widely scattered, intense thundershowers are common in the region.

Infrequent runoff that results from rapid snowmelt or from summer showers flows into ephemeral streams along the canyons and washes. Commonly, the beds of the washes are a mix of sand, gravel, and boulders, that rapidly absorb the infrequent flows. Most infiltrated water is returned to the atmosphere by evaporation and transpiration shortly after runoff ceases, but small quantities percolate to depths beyond which evaporation and transpiration are effective. This water ultimately recharges the ground-water system. A much larger proportion of the water in the ground-water flow system is recharged from precipitation northwest of the Yucca Mountain area. This water flows laterally to and beneath Yucca Mountain (Blankennagel and Weir, 1973, pl. 3; Winograd and Thordarson, 1975, pl. 1; and Rush, 1970, pl. 1). Migration of ground water from the area may be eastward locally, but ultimately is southward toward the Amargosa Desert.

Sass and Lachenbruch (1982, p. 16-25) concluded from geothermal data from wells at Yucca Mountain that water percolates with a downward component of flow through the unsaturated and saturated zones. They also concluded from calculated heat flows that the downward volumetric flow rate in the saturated zone may be about 1 to 10 mm/a, and the average water-particle velocity may be about 40 mm/a, assuming a porosity of 20 percent. Using an empirical method, Rush (1970, p. 15) used a precipitation-recharge rate for Yucca Mountain (computed from data for Jackass Flats, table 3 of this report) less than 5 mm/a. Rates for the horizontal component of flow were not estimated.

#### LITHOLOGY

Rocks penetrated by the well are mostly ash-flow tuff with various degrees of welding (table 1), as determined from bit cuttings and from geophysical-log correlations with nearby test well USW G-3 (fig. 1). The principal exceptions in the tuff sequence are four thin, poorly lithified, bedded, or reworked tuffs at the bases of several stratigraphic units.

Table 1.--Generalized lithologic log for test well USW H-3  
 [Modified from Thordarson and others (1984)]

Depth (meters)	Thickness (meters)	Stratigraphic unit	Lithology	
<u>Paintbrush Tuff:</u>				
0-	120	120	Tiva Canyon Member	Tuff, ash-flow, gray and orange, densely welded to nonwelded.
120-	123	3	Bedded tuff	Tuff, airfall, bedded, brown and gray, vitric and zeolitized(?); mostly pumice fragments.
123-	424	301	Topopah Spring Member	Tuff, ash-flow, mostly brown and orange, mostly moderately to densely welded, commonly devitrified.
<u>Rhyolite lavas and tuffs of Calico Hills (undivided):</u>				
424-	453	29	Tuffaceous beds of Calico Hills	Tuff, ash-flow(?), white to light gray; vitric; mostly pumice fragments.
<u>Crater Flat Tuff:</u>				
453-	579	126	Prow Pass Member	Tuff, ash-flow, pink, non-welded to partially welded, commonly devitrified.
579-	581	2	Bedded tuff	Tuff, bedded, reworked(?), yellow and pink, zeolitized(?); mostly pumice fragments.
581-	746	165	Bullfrog Member	Tuff, ash-flow, mostly brown, mostly densely welded, devitrified.
746-	755	9	Bedded tuff	Tuff, bedded, reworked, yellow and orange, zeolitized(?).
755-	1,096	341	Tram Member	Tuff, ash-flow, mostly gray, mostly partially welded, devitrified.
1,096-	1,109	13	Bedded tuff	Tuff, bedded, reworked, green.
<u>Lithic Ridge Tuff:</u>				
1,109-	1,219	110	-----	Tuff, ash-flow, gray, partially welded, partially zeolitic(?) and argillic(?).

The Tiva Canyon Member, the Topopah Spring Member of the Paintbrush Tuff, and the Bullfrog Member of the Crater Flat Tuff have the greatest degree of welding and are characterized as having mostly moderate-to-dense welding. The least welded tuffs are the Prow Pass Member of the Crater Flat Tuff, the Tram Member of the Crater Flat Tuff, the Lithic Ridge Tuff, and, perhaps, the Tuffaceous beds of Calico Hills, which are nonwelded to partially welded. A summary of welding characteristics and a detailed lithologic log of the penetrated rock are presented by Thordarson and others (1984).

Two geologic factors related to fracturing of the rock penetrated by the well are: (1) Older rocks would be expected to be more fractured because they have been exposed to more periods of mechanical stresses; and (2) densely welded rock is more brittle than less welded rock, and would be expected to break (rather than bend) from mechanical stress. The second factor probably dominates, in that the densely welded lithologic units probably are intensely fractured (Rush and others, 1984, p. 7). In the remainder of this report, stratigraphic members are referred to without reference to the formation of which they are a part; these relationships are given in table 1.

#### GEOPHYSICAL LOG INTERPRETATIONS

Sixteen types of geophysical logs were run in the well for a variety of purposes, including: (1) Defining lithology; (2) correlating with logs of other wells; (3) obtaining data for porosity, fractures, and permeability; (4) locating fluid level, casing perforations, and casing cement; and (5) gaging the diameter of the open-hole part of the well. Some of these uses are not discussed here because they do not directly contribute to characterization of the geohydrology of the penetrated stratigraphic units. However, they were useful in designing hydraulic tests for the well. A summary of the geophysical logs run in the well is given by Thordarson and others (1984).

Density, neutron, and 3-D velocity logs were used to determine the distribution of rock porosity, based on techniques described by Schlumberger Limited (1972, p. 37-55) and Birdwell Division (1973, p. OF90-OF188). The 3-D velocity log responds to matrix porosity. Borehole-compensated density and neutron logs respond both to matrix and fracture porosity. For the purpose of defining the general distribution of rock with greater-than-average porosity (that is, rock having porosity greater than the middle of the range indicated by the logs), the penetrated-rock sequence was divided into 80 equal-depth intervals, each about 15 m thick. Using the three types of logs, each depth interval was evaluated for percentage of relatively porous rock (that is, rock having porosity greater than the average for the entire sequence of rocks penetrated by the well). The three logs each produced results that were very similar, except for the interval 1,052 to 1,097 m in the lower part of the Tram Member, which had some differences between logs. The following conclusions are made from the resulting graph (fig. 2): (1) The Tuffaceous beds of Calico Hills, the lower part of the Tram Member, and the penetrated part of the Lithic Ridge Tuff are above average in porosity; (2) the four bedded tuffs are above average in porosity; and (3) thick intervals in the Topopah Spring and Bullfrog Members and the upper part of the Tram Member are below average in porosity.

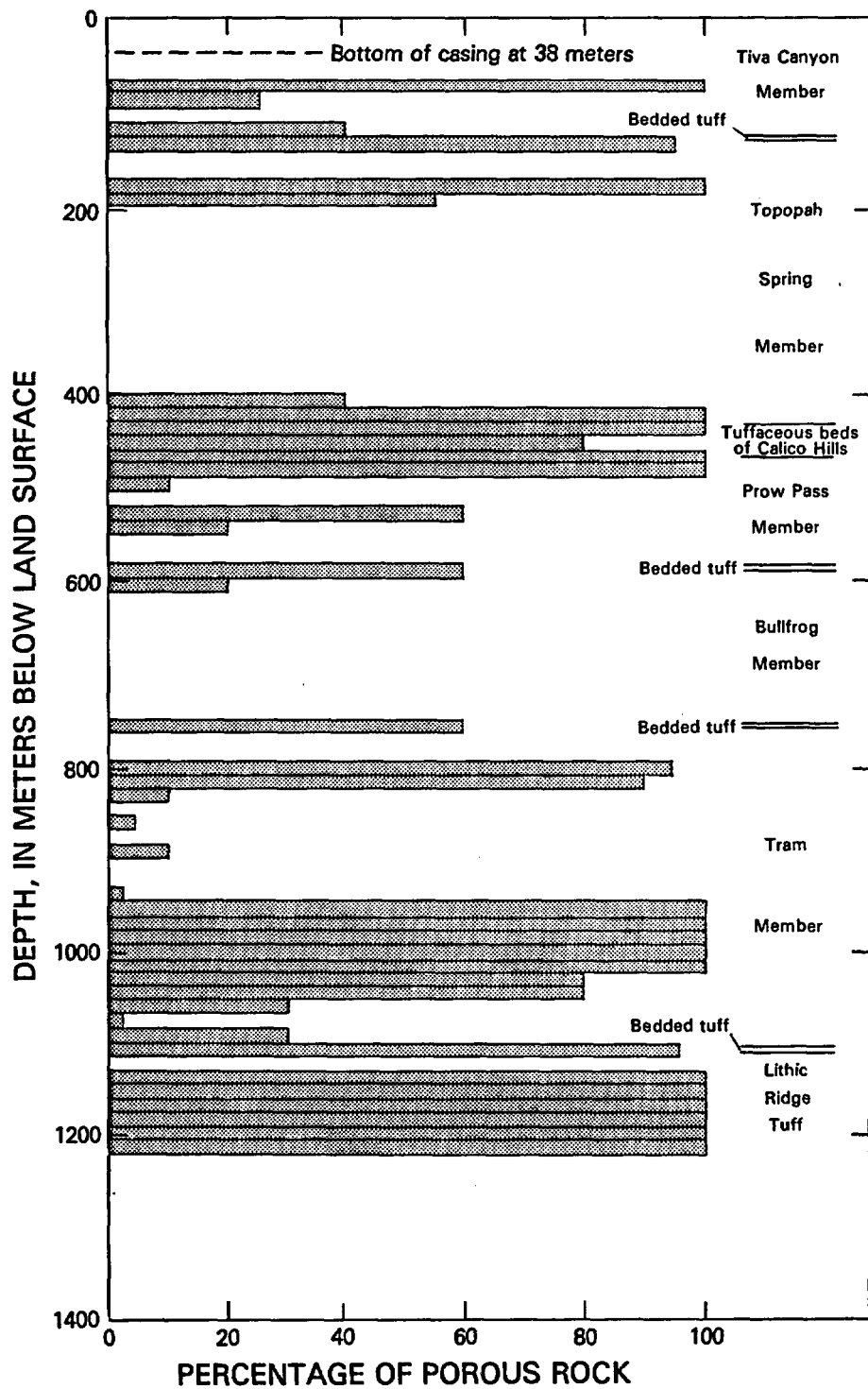


Figure 2.--Distribution of porous rock in the well, as determined from geophysical logs.

Porosity at shallow depth probably represents both matrix porosity and fractures. However, the volume of fracture porosity at greater depths probably is much less because of greater overburden pressure; therefore, the porosity represented there is largely or entirely matrix porosity.

The neutron log also can be used to determine the position of the water table. On February 19, 1982, while the well had a depth of 808 m and the slowly rising water level in the well was measured at a depth of 777 m, the water table could not be identified from the log. This may have been the result of the fracture and matrix porosity being so low that saturated rock below the water table had very little more water content than the overlying unsaturated rock, and the log could not measure the difference.

On July 23, 1982, 5 months after total depth was reached in test well USW H-3, a temperature log was made in the well under static logging conditions; that is, no stresses were applied to the well or the penetrated rock during the logging period and the water level was near static. However, effects of past drilling and testing stresses may have remained. A summary follows of some of the thermal conditions logged, or estimated from the log: (1) The estimated average ambient land-surface temperature at the well site was 25.3°C and the maximum recorded temperature in the well, at a depth of 1,211 m, was 43.3°C; (2) a temperature reversal occurred in the geothermal gradient, as recorded in the depth interval from 0 to 126 m, in the unsaturated Tiva Canyon Member; the lowest temperature in the well, 22.5°C, was at the base of this interval; and (3) the geothermal gradients in the unsaturated zone, 17.0°C/km, and in the saturated zone, 16.9°C/km, were very similar, suggesting that the difference in water content between the saturated and unsaturated zones was small.

The acoustic televiewer log, an acoustic traveltime log, was made to record borehole-wall texture in the liquid-filled part of the hole from the bottom of the casing at a depth of 792 m to a depth of 1,210 m. Such features as fractures and bedding planes were detected. Because the log is directionally oriented, the dip of inclined lineations was identified. Horizontal or nearly horizontal linear features were identified from the logs; they probably are either bedding planes or fractures. Steeply inclined linear features are more likely to be fractures. In the depth interval from 821 to 929 m, inclined linear features with mostly southwestward dips were identified. These features, probably fractures, had dips ranging from 60° to 80°. In the interval 1,029 to 1,107 m, another set of inclined linear features generally has dips to the northeast and east between 70° and 85°. Separating these two sets is an interval of 100 m of no detectable lineations. A listing of linear features is presented by Thordarson and others (1984).

Caliper logs were made during and after the drilling period to determine the open-hole diameter distribution with well depth. Erosion from drilling activity was the cause of the enlargement in well diameter. Erosion probably was caused by poor lithification, abundant fractures, and perhaps other unknown factors. Enlarged borehole zones that possibly were fracture controlled were identified by Thordarson and others (1984) from caliper logs as zones with irregular enlargement. The principal fracture-controlled zones are: (1) A thick interval (9 to 101 m) in the Tiva Canyon Member, and (2) a thick interval (169 to 358 m) in the Topopah Spring Member.

A television-camera log was made in the well before casing the well to a depth of 792 m. Open-hole conditions were logged from a depth of 38 m to the water level in the well at that time, 767 m. Features observed were fractures, hole enlargement, lithologic features, and a water seep. The fractures were observed at many depths, but mostly in the Tiva Canyon Member and the upper part of the Topopah Spring Member; they are listed by Thordarson and others (1984). Water was observed seeping from fractures, above static water level, at a depth of 277 m. Slickensides with lateral displacement were observed at a depth of 216 m in the upper part of the Topopah Spring Member.

#### BOREHOLE-FLOW SURVEY

A borehole-flow survey using a radioactive tracer (Blankennagel, 1967 and 1968) was used to measure vertical flow rates in the well, while water was pumped into the well at a rate of 2.7 L/s and with constant head. From this measurement, the zones through which the water flowed from the well and estimated flow rates for the zones were identified. The survey was made after the well had been cased to a depth of 792 m and had a total depth of 1,219 m. The units tested included the saturated lower 308 m of the Tram Member and the penetrated underlying units (fig. 3).

Conclusions from the survey, assuming no significant hydraulic-head loss in the wellbore are:

1. In the 31.9-m interval from 809 to 840.9 m, about 7 percent of the surveyed interval received 63 percent of the injected water. This interval is in the upper part of the Tram Member.
2. The second greatest injection rate was for the interval from 1,060 to 1,120.4 m, about 14 percent of the surveyed interval, extending from the lower part of the Tram Member through bedded tuff and into the upper part of the Lithic Ridge Tuff. This interval received 30 percent of the flow.
3. The small remaining part of the total flow mostly entered the interval from 840.9 to 933 m of the Tram Member. The other intervals received little, if any, of the flow.

In a later section of this report, these survey results are used in conjunction with hydraulic tests to assign values of transmissivity and hydraulic conductivity to 28 intervals within the saturated zone.

#### WATER-LEVEL MONITORING

Water-level observations and measurements in the well were made during the drilling period, as part of hydraulic tests, and after testing was completed. The purposes of these observations and measurements were: (1) To locate any perched-water zones above the water table, (2) to identify the depth at which water saturation occurs, (3) to determine the composite hydraulic head in the well, (4) to identify hydraulic heads in various water-bearing zones, and (5) to determine the existence of artesian or water-table conditions.

TD  
1219 m

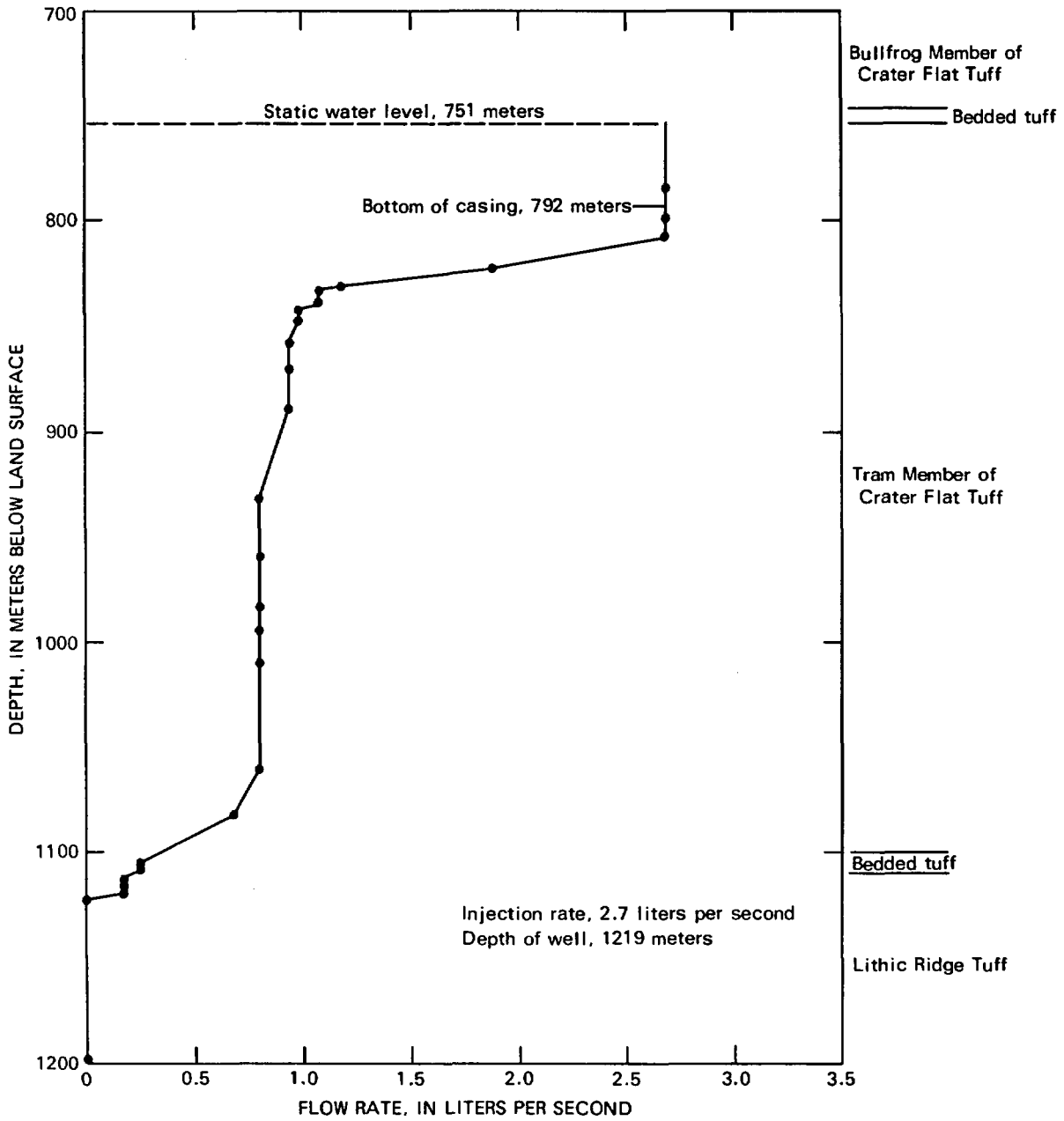


Figure 3.--Borehole-flow survey for test well USW H-3 (modified from Thordarson and others, 1984, p. 19).

During drilling of the interval from 744 to 753 m, either perched ground water or returning drilling fluid entered the well from the rock. If it was ground water, the likely source was ash-flow tuff at the base of the Bullfrog Member. This unit overlies a bedded tuff, depth interval from 746 to 755 m. Later, the composite-hydraulic head in the well stabilized at a depth of  $750.7 \pm 0.2$  m below land surface (Thordarson and others, 1984). Below the bedded tuff, the Tram Member and all underlying units were saturated and possibly under artesian conditions in the vicinity of the well, similar to conditions at test well USW H-1 (Rush and others, 1984).

To obtain information on the vertical distribution of hydraulic head at the well, a packer was installed at a depth of 1,190 m. On November 3, 1983, the hydraulic head in the rocks above the packer was at 732.9 m above sea level; below the packer, the head in those rocks was at 754.0 m above sea level and rising slowly toward static conditions. These results indicate that the lower zone had a composite head at least 21.1 m higher than the upper zone.

#### HYDRAULIC TESTING

This section of the report includes descriptions of pumping-, injection-, and swabbing-test results. The tests were made following the drilling of the well to final depth. Test results are discussed separately in subsequent sections of the report. Following these sections, results from the three types of tests are compared, differences reconciled, and representative values selected for various depth intervals in the penetrated part of the saturated zone.

According to Bredehoeft and Maini (1981, p. 293-294), definition of ground-water flow and the parameters that control flow through typical porous media--sand, gravel, sandstone--are well understood. In contrast, flow through a fractured-rock mass, such as tuffs beneath Yucca Mountain, is much less understood. Neither the theory nor the field technology required to measure flow characteristics of a ground-water system in a fractured medium is very advanced; thus, uncertainties in predictions are great in both time and space. As a result, in the following paragraphs, a conceptual model of the ground-water system beneath Yucca Mountain is presented and a solution to the theory and field-technology dilemma is proposed.

To define ground-water parameters for the flow system at this well site, a conceptual model is desired. The principal elements of the model are those of Rush and others (1984):

1. The rock is nearly homogeneous and isotropic. Primary porosity is intergranular and controlled in ash-flow tuffs principally by degree of welding and degree of alteration.

2. Secondary porosity is controlled by fractures. These fractures generally are vertical or at a steep angle and may be spatially random in the saturated zone (Baecher, 1983, p. 329), and are the result of tensional and shear failure during mechanical deformation during tectonic activity or fracturing during cooling. The volume of water stored in fractures is relatively small in comparison to that stored in the matrix porosity. On a small

scale, the tectonic fracture permeability is anisotropic. However, the fracture permeability due to cooling joints probably would be isotropic in plan view, as well as homogeneous, because only random fracture strikes would be observed (Scott and others, 1983, p. 315).

3. Both primary and secondary porosity may be decreased by precipitation of minerals.

4. Flow to the well is through the fracture network only; however, flow probably occurs between pores and fractures. Hydraulic conductivity of fractures is several orders of magnitude larger than hydraulic conductivity of the matrix.

5. Distances between fractures are small in comparison with the dimensions of the ground-water system under consideration.

6. In ash-flow tuffs, zones of approximately the same degree of welding have approximately the same density of fracturing (Scott and others, 1983, p. 309). Sufficiently dense fracture spacing probably results in the fractured ash-flow tuffs functioning in a hydraulically similar fashion to a granular porous medium (Freeze and Cherry, 1979, p. 73).

Based on the conceptual model, homogeneous porous-media solutions can be used to define general ground-water parameters and ground-water flow in fractured media, using late-time test data to define this dual-porosity system (Warren and Root, 1963; Odeh, 1965; Kazemi, 1969; Kazemi and Seth, 1969; Wang and others, 1977, p. 104; and Najurieta, 1980, p. 1242). However, early-time test data will yield parameters that apply only to the fractured part of the system. Data used for computing apparent transmissivity for all types of tests in this well probably are early-time data, as concluded by Rush and others (1984) for test well USW H-1, and therefore apply only to the fractured part of the system. The earliest hydraulic-head-change data may be dependent partly on nonrepresentative, near-well hydraulics (Wang and others, 1977, p. 103), on wellbore storage, and on skin effects. During pumping, skin effect is the pressure drop at the wellface in addition to the normal transient pressure drop in the ground-water system resulting from damage or improvement of the rock's ability to transmit water at the wellface (Earlougher, 1977, p. 57). Commonly, the damage or improvement is the result of well drilling.

Witherspoon and others (1980, p. 26-28), in their hydrologic work in crystalline rock, have assumed that, in general, a fracture system can be treated as a slightly different form of porous medium, measuring equivalent porous-media properties. The porous-media solutions will not yield correct porosity and hydraulic-conductivity values for each matrix or fracture porosity type in this dual-porosity system beneath Yucca Mountain, but rather average values for the zones tested. As a result, hydraulic conductivity, aperture, and volume of specific fractures or effective pore volume of the matrix are not determined.

The degree of reliability of the conceptual model is related to the degree to which the model approximates the actual fracture-flow ground-water system beneath Yucca Mountain, for the purposes intended and for the time during which the data are valid. The departure of test data is a measure of how far conditions are from the ideal (Ferris and others, 1962, p. 102). Departure from ideal for each test has been evaluated and is described in the following sections where testing results are presented and in table 2.

TD 1219 m

Table 2.--Summary of test results

Test interval (meters)	Transmissivity (meters squared per day)	Storage coeffi- cient	Departure of data from ideal	Remarks
<u>PUMPING TESTS</u>				
754-1,219 (fig. 4)	$5 \times 10^{-1}$	-----	Small	Using second cycle of pumping.
754-1,219 (fig. 5)	$4 \times 10^{-1}$	-----	Small	Using all cycles of pumping.
<sup>1</sup> 822-1,219 (fig. 6)	1.0	-----	Small	Long-term test.
<u>INJECTION TESTS</u>				
792- 850 (fig. 13)	1.2	$4 \times 10^{-6}$	Moderate	Using slug-test method of analysis.
851- 917 (fig. 14)	$2 \times 10^{-2}$	-----	Small	Using straight-line method of analysis.
911- 972 (fig. 15)	$3 \times 10^{-2}$ $6 \times 10^{-2}$	----- $6 \times 10^{-6}$	Large Moderate	Do. Using slug-test method of analysis.
972-1,219 (fig. 16)	$1 \times 10^{-1}$ $3 \times 10^{-2}$	$7 \times 10^{-6}$ -----	Moderate Large	Do. Using straight-line method of analysis.
1,063-1,124 (fig. 17)	$3 \times 10^{-2}$	-----	Large	Used straight-line method of analysis.
	$1 \times 10^{-1}$	$7 \times 10^{-6}$	Large	Used slug-test method of analysis.
1,126-1,219 (fig. 18)	$1 \times 10^{-2}$	-----	Small	Used straight-line method of analysis.
<u>SWABBING TESTS</u>				
792-1,219 (fig. 19)	1.1	-----	Small	Used straight-line method of anal- ysis.
1,063-1,124 (fig. 20)	$1 \times 10^{-1}$	-----	Small	Do.

<sup>1</sup>Pumping zone below a packer.

### Pumping Tests

The well was initially and briefly pumped for several cycles of drawdown and recovery, using a submersible pump. The well could not sustain the yield of several liters per second. The brief drawdowns and recoveries of the water level were measured to determine transmissivity of the part of the saturated zone penetrated by the well (figs. 4 and 5). Later, a smaller pump was used, which discharged at a rate of 0.16 L/s (fig. 6). Because a large volume of water was not pumped from the well, no representative samples of ground water were collected for chemical analyses.

The methods used to analyze the data were the straight-line method (Cooper and Jacob, 1946; Ferris and others, 1962, p. 100), Brown's method (Ferris and others, 1962, p. 122), and the Theis method (Lohman, 1972, p. 15). Method assumptions are discussed in the cited references. Results of these and other tests are discussed and summarized in table 2.

For the straight-line method of analysis of the recovery in a pumped well, residual drawdown,  $s'$ , was plotted against time after pumping started, divided by time after pumping stopped,  $t/t'$ , on semilogarithmic-coordinate scale. After values of time became sufficiently large, and after testing conditions were met (as described earlier in this report), the measured data plotted along a straight line. The slope of this line for one log cycle,  $\Delta s'$ , was used in the following equation:

$$T = \frac{15.8Q}{\Delta s'} , \quad (1)$$

where

$T$  is transmissivity, in meters squared per day;  
 $Q$  is constant rate of discharge of the well, in liters per second; and  
 $s'$  is residual drawdown for one log cycle, in meters.

A transmissivity of  $5 \times 10^{-1} \text{ m}^2/\text{d}$  was computed in figure 4 using a single cycle of the initial pumping period.

For Brown's method, drawdown and recovery,  $s$ , were plotted against time after pumping started,  $t$ , on arithmetic-coordinate paper. Then, the intervals of time between the start of pumping in each cycle and the end of the final recovery period were calculated, resulting in values for  $t_1$  through  $t_5$ . The intervals of time between the end of the recovery period in each cycle and the end of the final recovery period were calculated, resulting in values for  $t'_1$  through  $t'_5$ . Then, these values of  $t$  and  $t'$  were substituted into Brown's equation:

$$T = \frac{15.8Q}{s_5} \left[ \log \left( \frac{t_1}{t'_1} \right) \left( \frac{t_2}{t'_2} \right) \left( \frac{t_3}{t'_3} \right) \left( \frac{t_4}{t'_4} \right) \left( \frac{t_5}{t'_5} \right) \right] , \quad (2)$$

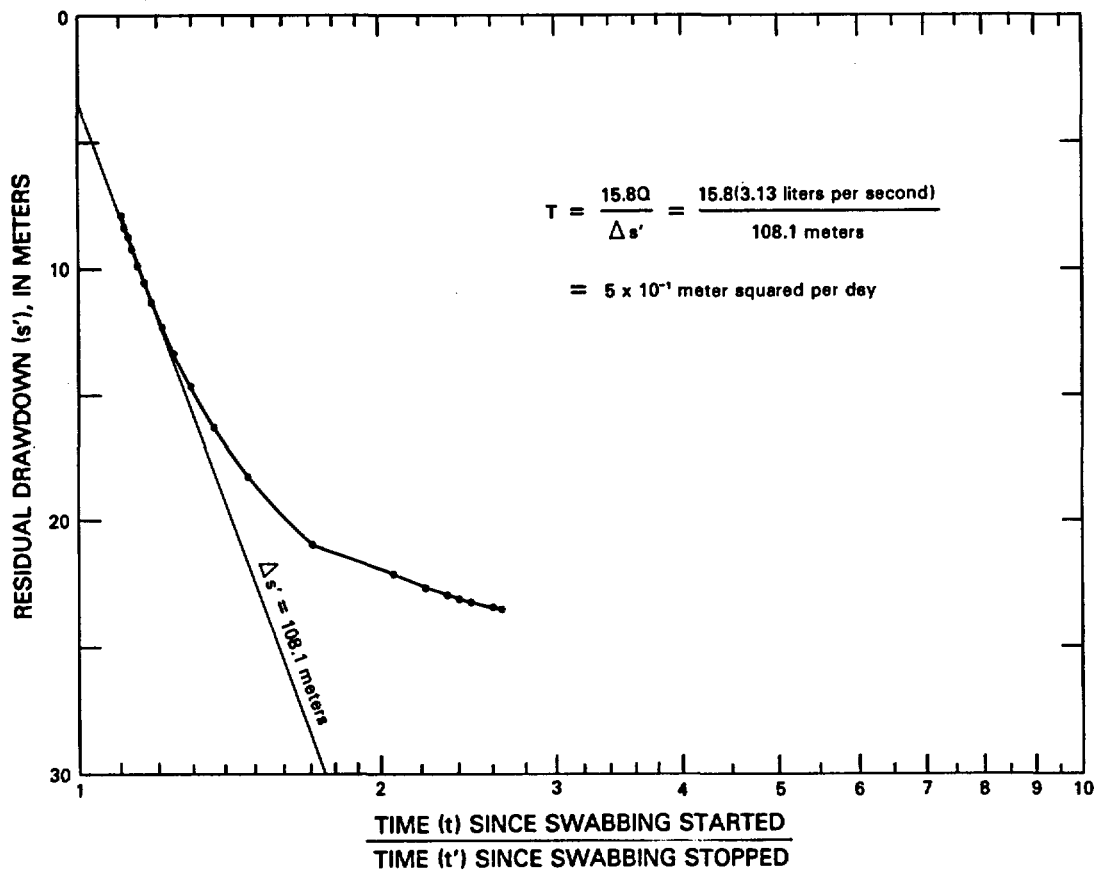
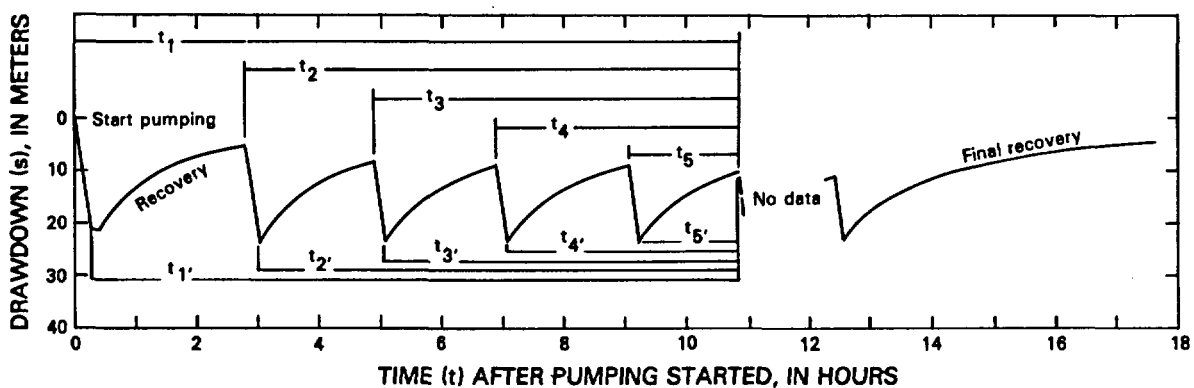


Figure 4.--Analysis of water-level recovery following second cycle of pumping of the interval from 754 to 1,219 meters, using the straight-line method.



$$T = \frac{15.8(2.84 \text{ liters per second})}{11.1 \text{ meters}} \log \left( \left( \frac{643.4 \text{ minutes}}{628.4 \text{ minutes}} \right) \left( \frac{483.4}{466.4} \right) \left( \frac{355.8}{344.8} \right) \left( \frac{236.8}{226.3} \right) \left( \frac{108.5}{98.2} \right) \right) = 4 \times 10^{-1} \text{ meter squared per day}$$

Figure 5.--Analysis of the pumping test of the interval from 754 to 1,219 meters, using Brown's method for a cyclically pumped well.

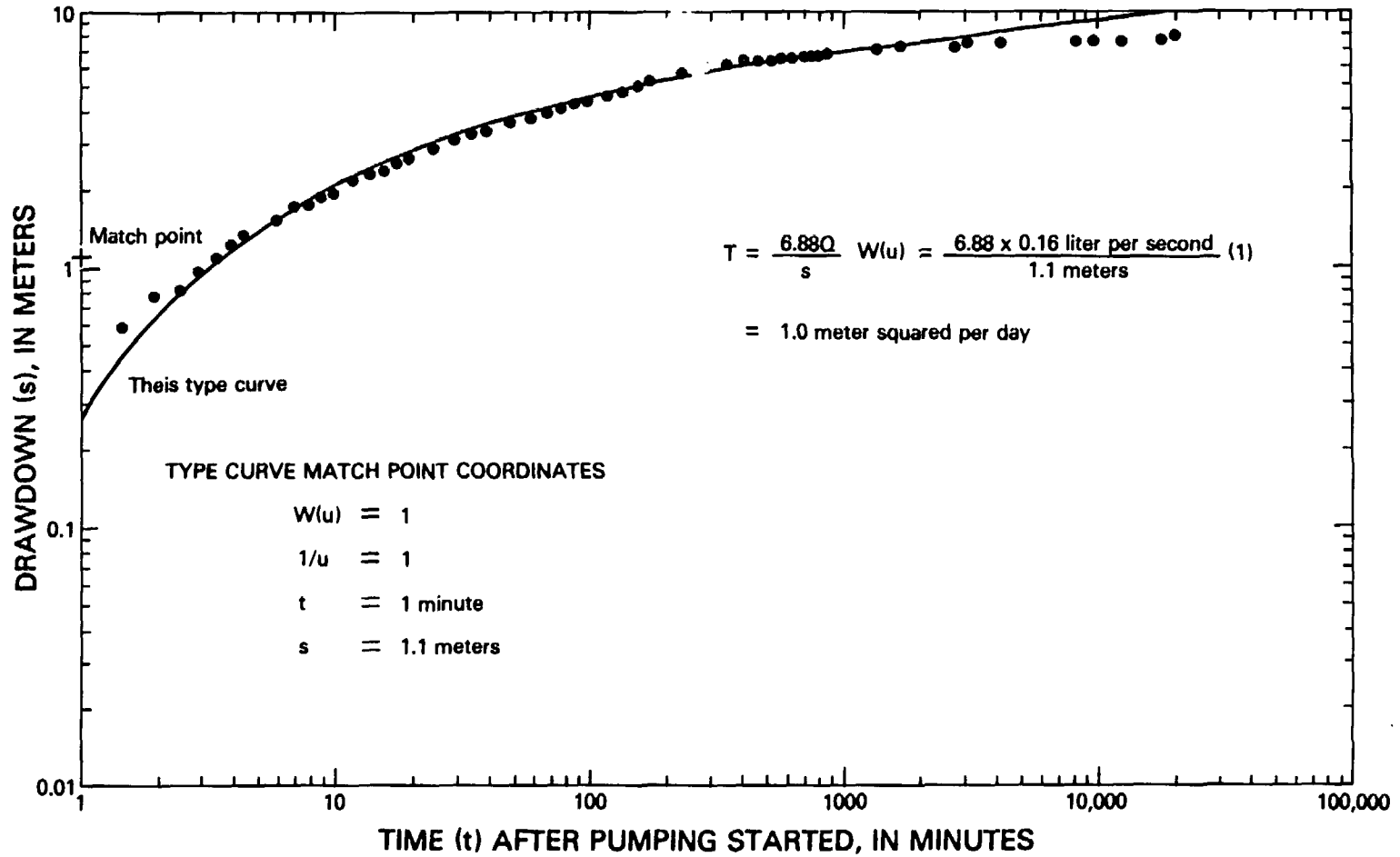


Figure 6.--Analysis of water-level drawdown of the interval from 822 to 1,219 meters, using the Theis method.

where

T is transmissivity, in meters squared per day;  
Q is constant rate of discharge, in liters per second; and  
 $s_5$  is net drawdown at the end of the fifth cycle, the last cycle used, in meters.

A transmissivity of  $4 \times 10^{-1} \text{ m}^2/\text{d}$  was computed in figure 5 using multiple cycles of the initial pumping period.

For the Theis method, drawdown,  $s$ , was plotted against time after pumping started,  $t$ , on logarithmic-coordinate paper. The data curve then was superimposed on a type curve to obtain the best fit of the data to the type curve. An arbitrary match-point was selected anywhere on the overlapping part of the sheets, and the four coordinates of common point on the two sheets were determined. The following equation then was used:

$$T = \frac{6.88 Q}{s} W(\mu), \quad (3)$$

where

T is transmissivity, in meters squared per day;  
Q is constant rate of discharge, in liters per second;  
 $W(\mu)$  is well function, a match-point coordinate; and  
 $s$  is drawdown in meters, another match-point coordinate.

Later, in January 1984, a long-term, small-discharge-rate pumping test was made testing the interval from a packer installed at a depth of 822 m to a depth of 1,219 m. The resulting data (fig. 6) yields a transmissivity of about  $1.0 \text{ m}^2/\text{d}$ . This interval is 85 percent of the penetrated part of the saturated zone, the packer being set about 71 m below the composite static-water level. The data curve strongly resembled the results of pumping test 2, zone from 687 to 1,829 m in test well USW H-1 (Rush and others, 1984, fig. 12), farther north on Yucca Mountain (fig. 1). The departure of the data curve from the type curve at time 2,500 minutes indicates leaky aquifer conditions, that a recharging boundary had been reached by the cone of depression caused by pumping, or that the transition from early time to late time was reached. The discharge rate was about 0.16 L/s and the maximum drawdown was 8.12 m for the 20,520-minute pumping period. Pumping-test results analyzed in figures 4, 5, and 6 have only small departures from ideal.

### Injection Tests

Injection tests were made in selected depth intervals by using inflatable packers in the well to isolate the test zones. Injection-test data were analyzed by the straight-line method described for pumping tests earlier in this report and the slug-test method described by Cooper and others (1967) and Papadopoulos and others (1973). The assumptions are discussed in the cited references. Six tests were successfully completed.

For the slug-test method of analysis, the ratio of hydraulic head at a given time to hydraulic head at time zero,  $H/H_0$ , was plotted against time after injection started,  $t$ , on semilogarithmic-coordinate paper.  $H/H_0$  was plotted on the arithmetic scale; time was plotted on the logarithmic scale. A family of type curves was used to determine transmissivity and storage coefficient. A match point was selected on the logarithmic scale of the type-curve graph, with a value of 1.0. The corresponding time,  $t$ , match point on the logarithmic scale of the data graph was determined. The following equation then was used to calculate transmissivity:

$$T = \frac{1.0 r_c^2}{t}, \quad (4)$$

where

$T$  is transmissivity, in meters squared per day;  
 $r_c$  is radius of the tubing used in the packer assembly, in meters; and  
 $t$  is the match-point time, in days.

To estimate the coefficient of storage,  $S$ , the following equation was used:

$$S = \frac{r_c^2}{r_s^2} \alpha \quad (5)$$

where

$\alpha$  is the recorded matching curves value; and  
 $r_s$  is the radius of the open hole, in meters.

Use of early injection-test data to determine aquifer properties will give erroneous results because of wellbore-storage effects and hydraulic-fracturing effects. These effects are discussed in the following paragraphs.

Wellbore-storage effects were prominent during the early parts of the injection tests as a result of a gradually changing rate of injection at the formation face. During the early part of the injection, the large injection rate into the formation probably represents water being released from storage in the tubing; the later part of the injection, when the injection pressure and rate were less, represents more accurately the rate of injection at the formation face. During wellbore-storage domination, a full logarithmic plot of change of pressure versus change in time shows a unit slope of one cycle of pressure change per one cycle of time change; this unit slope represents data that cannot be used to analyze formation properties (Earlougher, 1977).

Effects of wellbore storage that were prominent during early parts of the injection tests were identified by drawing a unit-slope straight line on log-log plot of  $\Delta p$  and  $t$ , as shown in figures 7 and 8 (Earlougher, 1977). This plot shows the dominance of wellbore-storage effects during the first 3 minutes of the tests. The data following departure from unit slope are analyzed for transmissivity.

Hydraulic-fracturing effects probably occurred during the early parts of the injection tests because of the large hydraulic head exerted. Effects of probable widening of fractures during the first 5 to 6 minutes were found in the double-humped curves for the injection tests in figures 14 to 18 presented later in this section. However, the test for the interval from 792 to 850 m showed a more normal S-shaped curve as presented in figure 13 later in this section. The brief widening of fractures was caused by the great height of the column of water in the tubing, amounting to about 750 m above the static water level. At a pressure gradient of 9.80 kPa/m for fresh water, a column of 750 m exerted a total instantaneous bottom-hole pressure of  $7.4 \times 10^3$  kPa, a pressure that exceeds the pressure that is needed to produce vertical fractures in a tectonically relaxed geologic environment (Hubbert and Willis, 1972). For example, pressure needed to produce hydraulic fractures in dolomites in New York is only  $6.6 \times 10^3$  kPa (Waller and others, 1978, p. 29). A plot of pressure versus injection rate for the tests in test well USW H-3 is presented in figure 9 to show the nearly flat slope that is indicative of hydraulic widening of fractures, a method used for the fractured dolomites in New York. Injection-test data generally show a nearly flat slope from approximately 2 to 5 minutes, except for the injection test for the interval from 792 to 850 m. That test shows a more normal inclined slope. The nearly flat slopes are attributed to widening of fractures with associated transient increases in transmissivity.

Possible fracture widening from hydraulic pressure also is indicated by plots of velocity of the injection of water versus time shown in figures 10 and 11, and specific capacity versus time, as shown in figure 12. The plots of velocity versus time in figures 10 and 11 have steep slopes for tests with hydraulic-fracture widening; after 10 to 18 minutes the velocity decreases to less than 2.2 m per minute, a velocity below which turbulent flow in the tubing probably ends. This velocity may indicate when the turbulence in the fracture changes to laminar flow. The plot of specific capacity versus time (fig. 12) indicates fracture widening between 2 to 5 minutes by the very steep slope of the curve. Specific capacity becomes more uniform and unchanging after approximately 7 to 9 minutes for injection tests with fracture widening, and after 70 minutes for the test of the interval 792 to 850 m, which does not show fracture widening; the data are analyzed best after the specific capacity becomes more uniform.

The data for injection tests shown in figures 13 through 18 are very much affected by wellbore-storage and fracturing effects. These effects are present in the early-time data during the first 5 to 7 minutes; as a result, this part of the data curve will give erroneous results if used in calculating hydraulic properties.

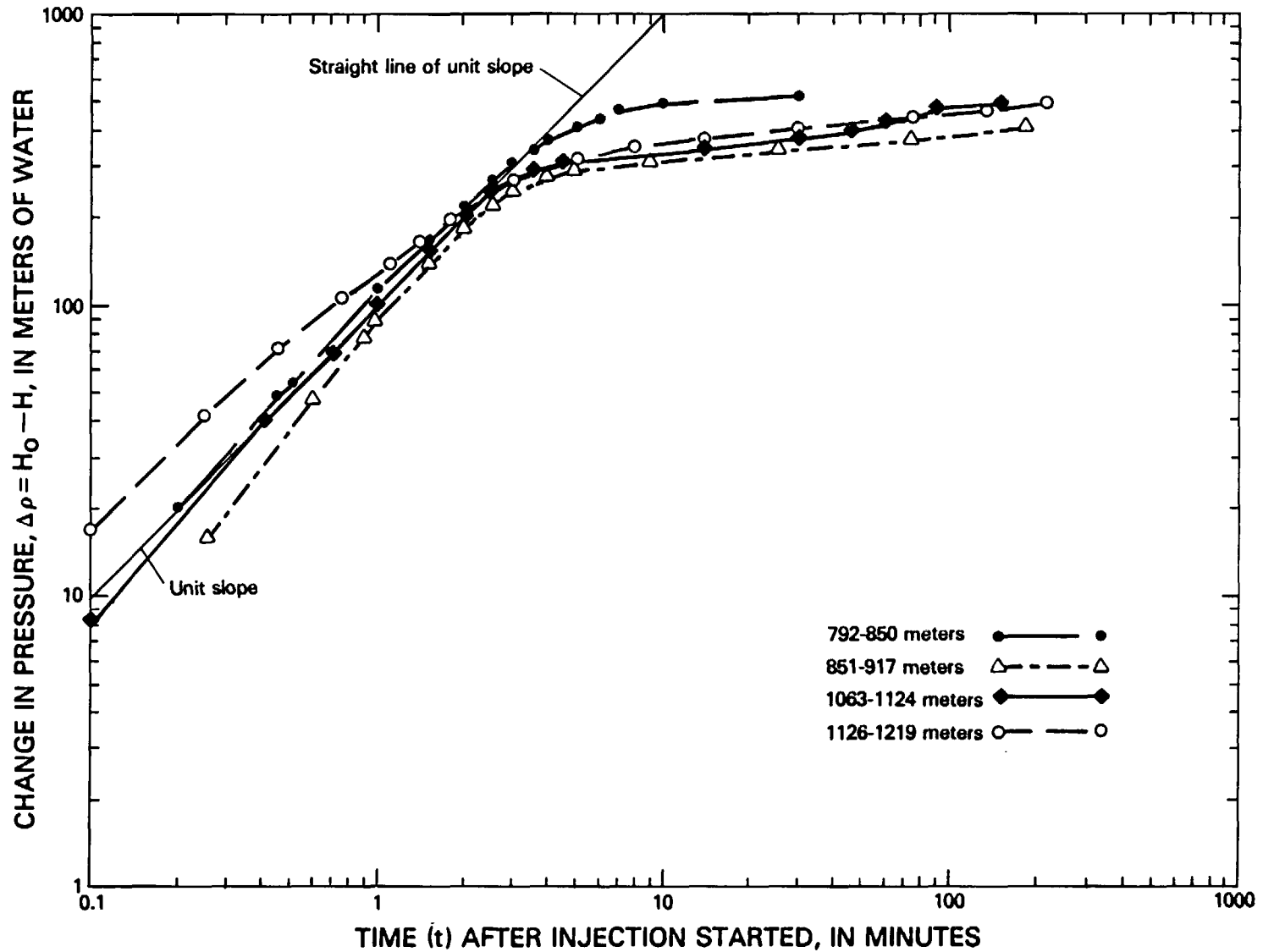


Figure 7.--Wellbore-storage effects during injections tests of the intervals from 792 to 850, 851 to 917, 1,063 to 1,124, and 1,126 to 1,219 meters.

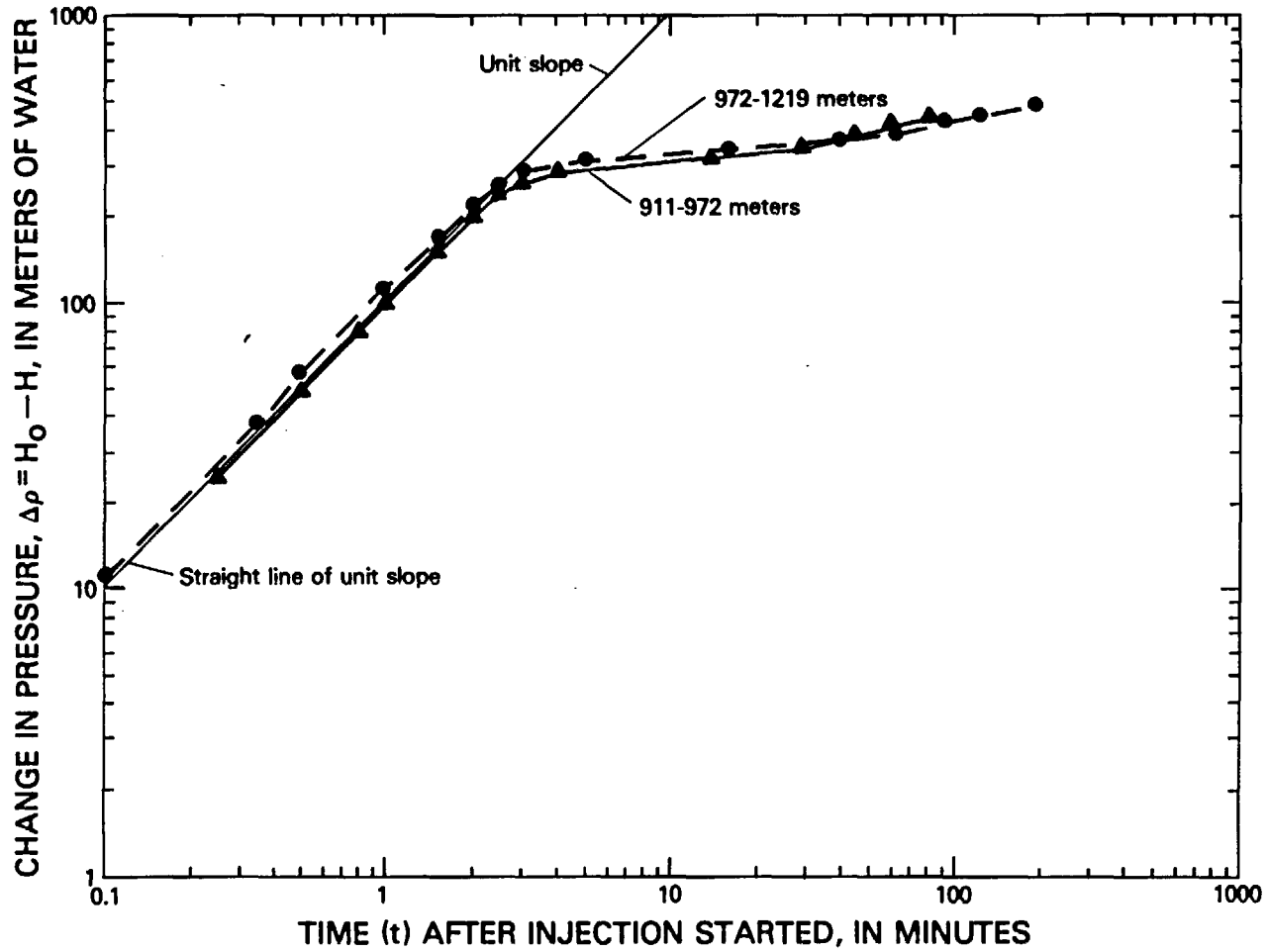


Figure 8.--Wellbore-storage effects during injection tests of the intervals from 911 to 972 and 972 to 1,219 meters.

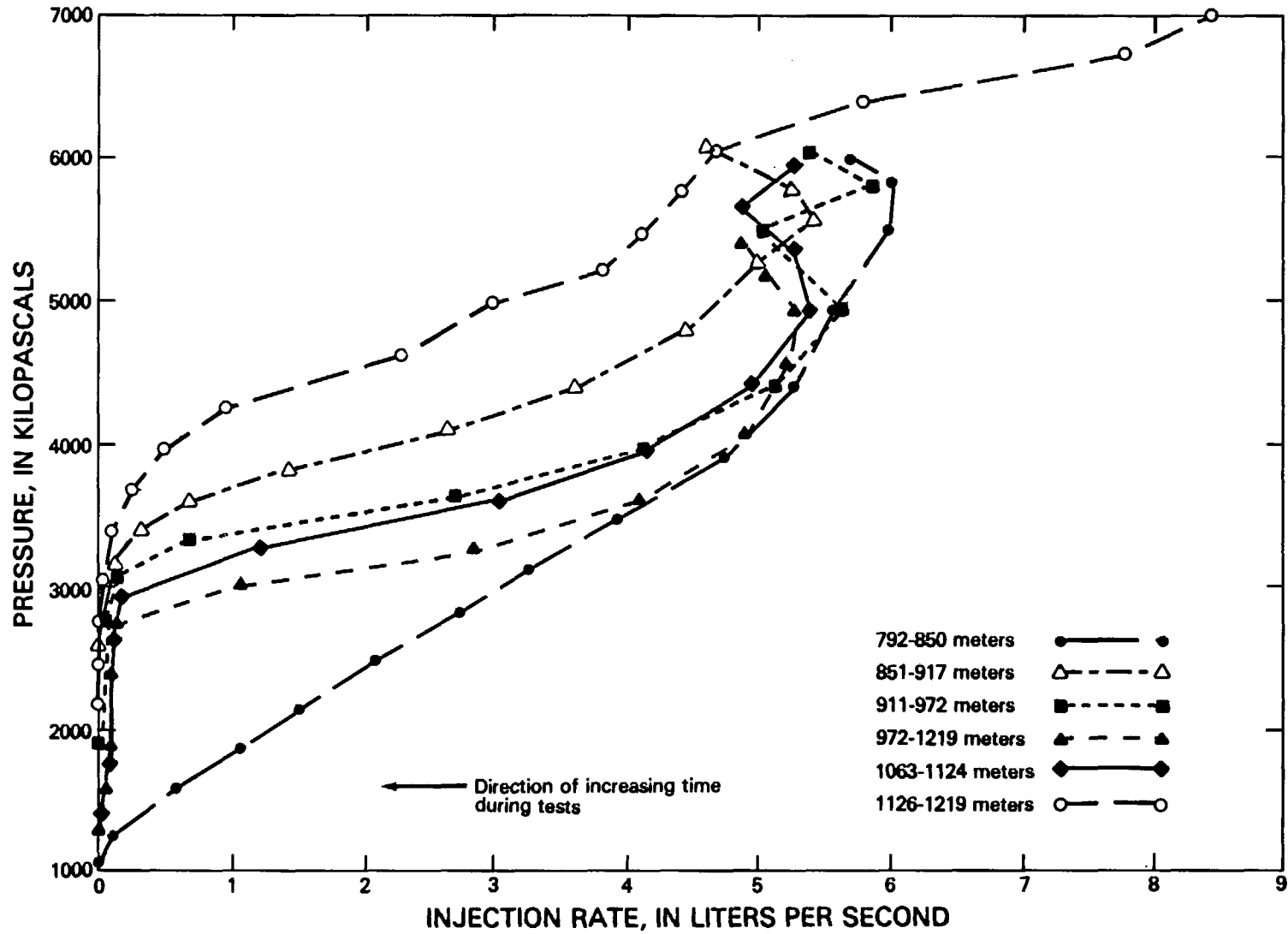


Figure 9.--Relation of pressure and injection rate during injection tests.

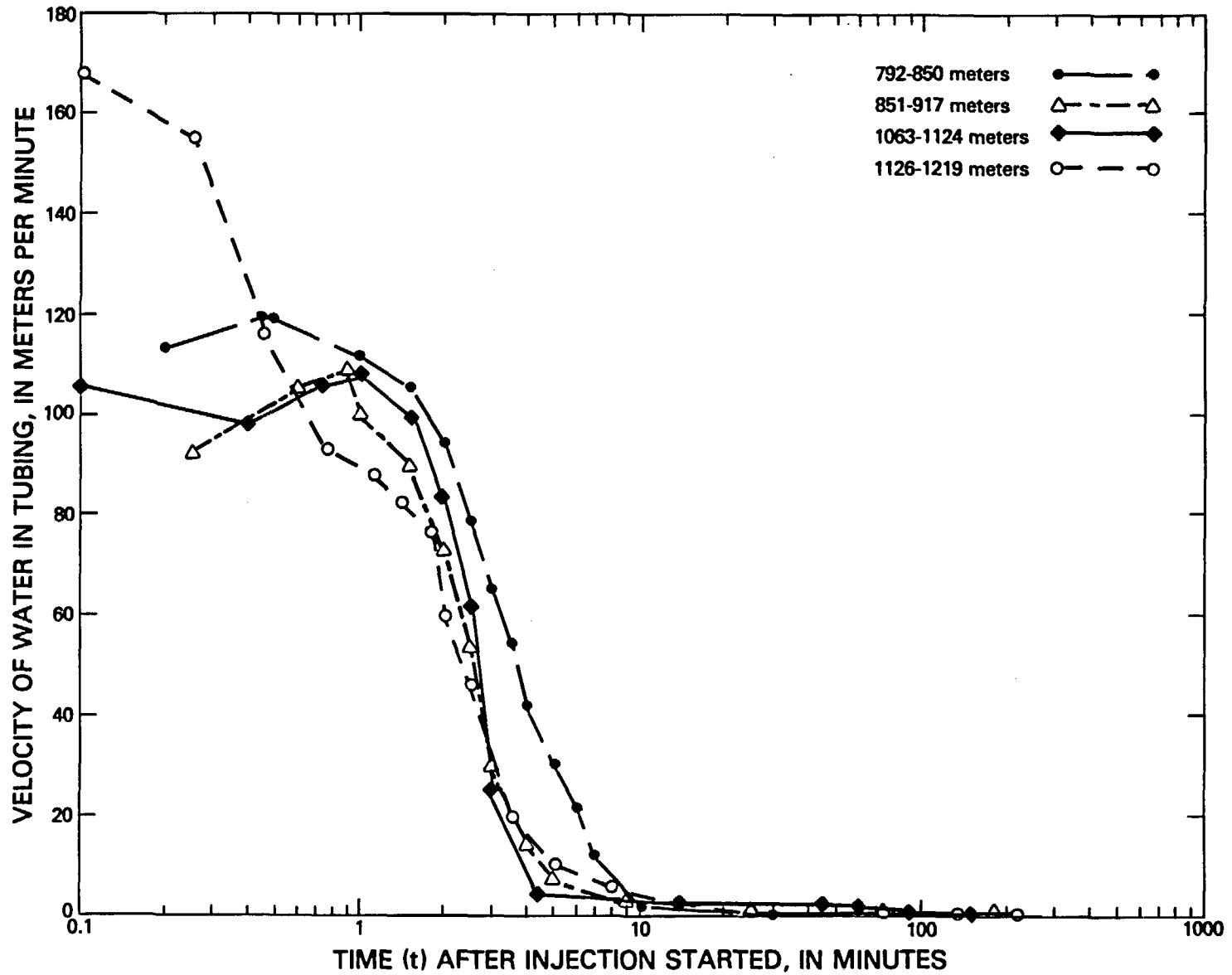


Figure 10.--Velocity of water in tubing during injection tests of the intervals from 792 to 850, 851 to 917, 1,063 to 1,124, and 1,126 to 1,219 meters.

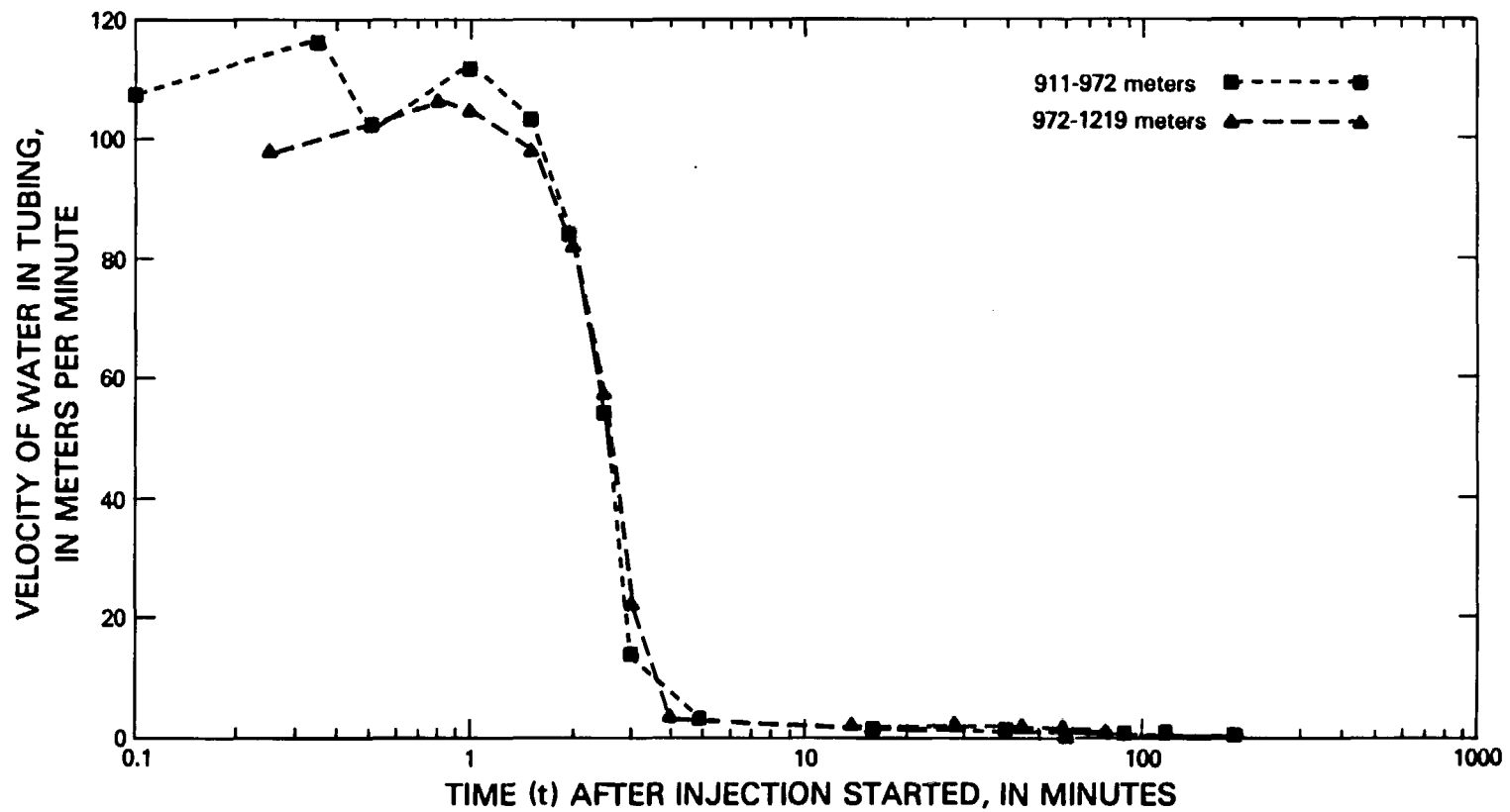


Figure 11.--Velocity of water in tubing during injection tests of the intervals from 911 to 972 and 972 to 1,219 meters.

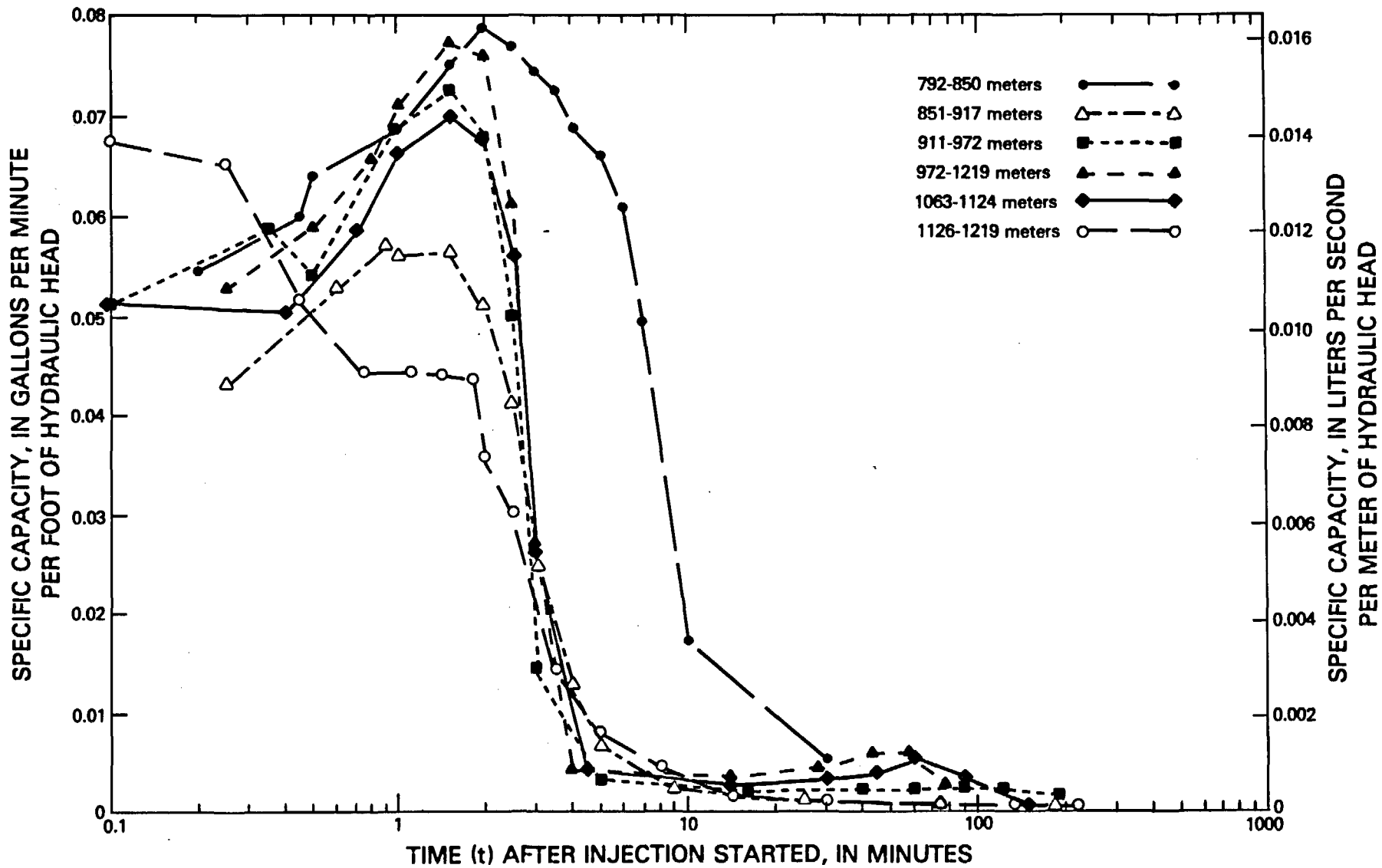


Figure 12.--Relation of specific capacity and time during injection tests.

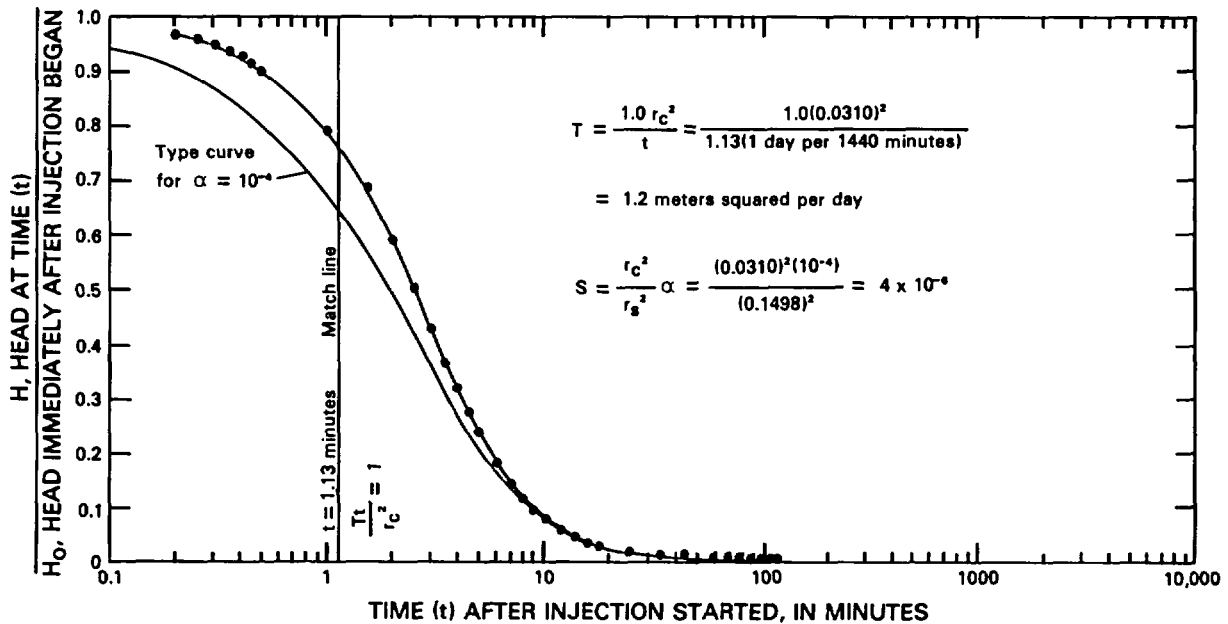


Figure 13.--Analysis of injection test of the interval from 792 to 850 meters, using the slug-test method.

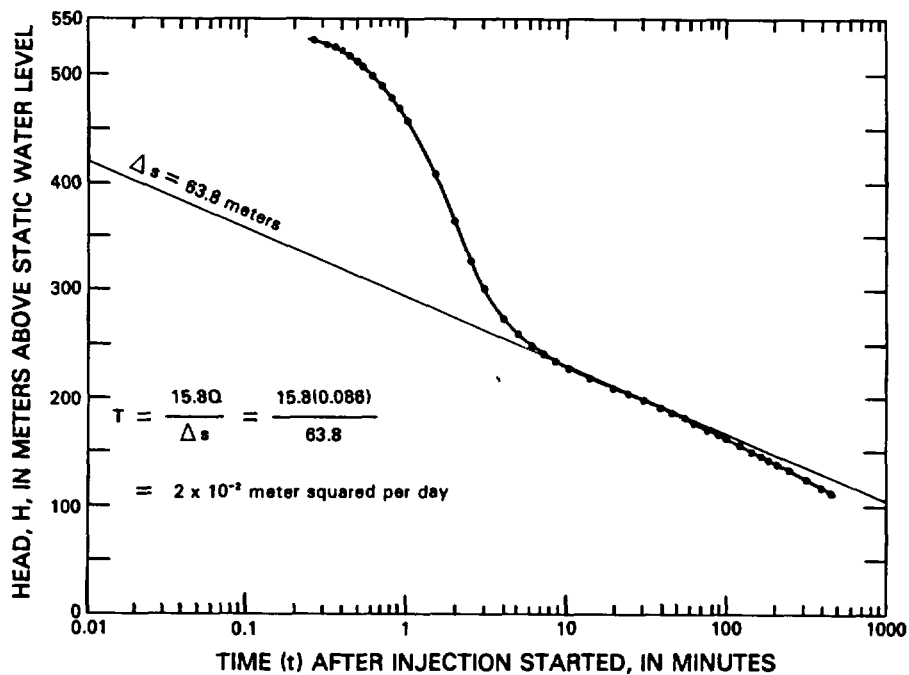


Figure 14.--Analysis of injection test of the interval from 851 to 917 meters, using the straight-line method.

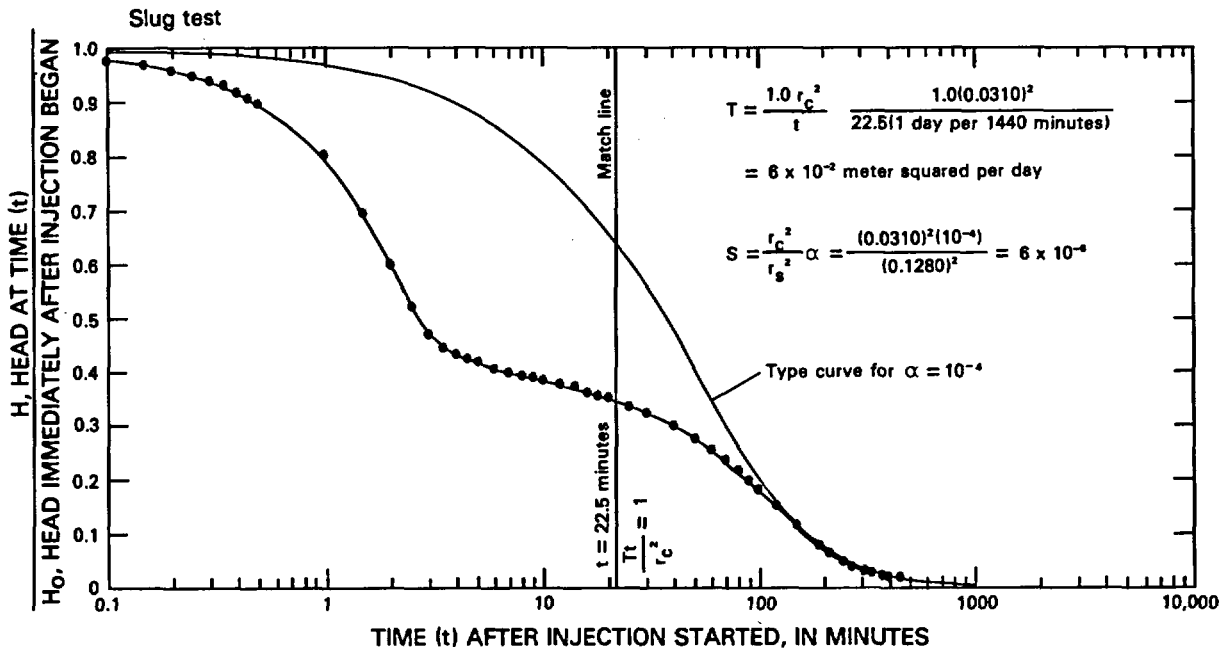
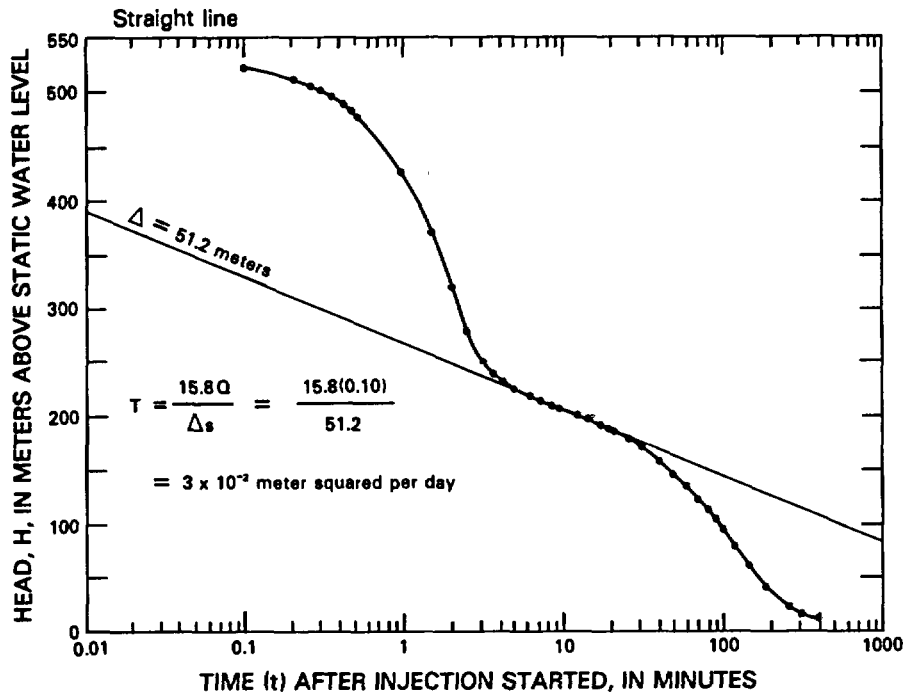


Figure 15.--Analysis of injection test of the interval from 911 to 972 meters, using straight-line and slug-test methods.

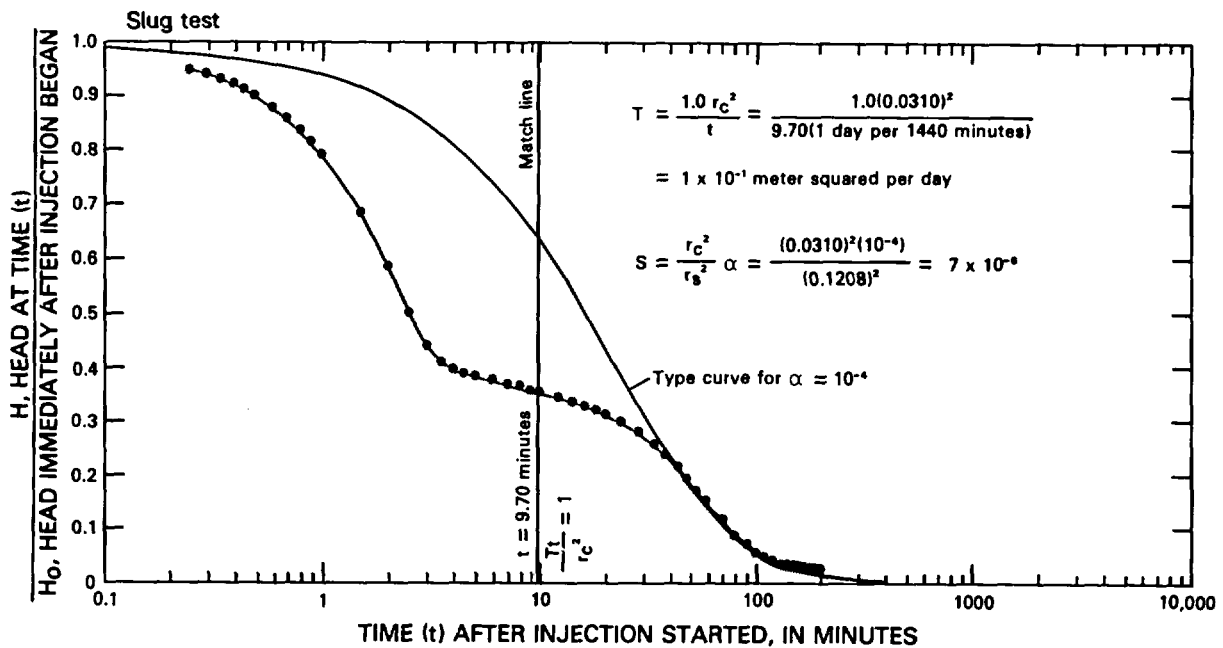
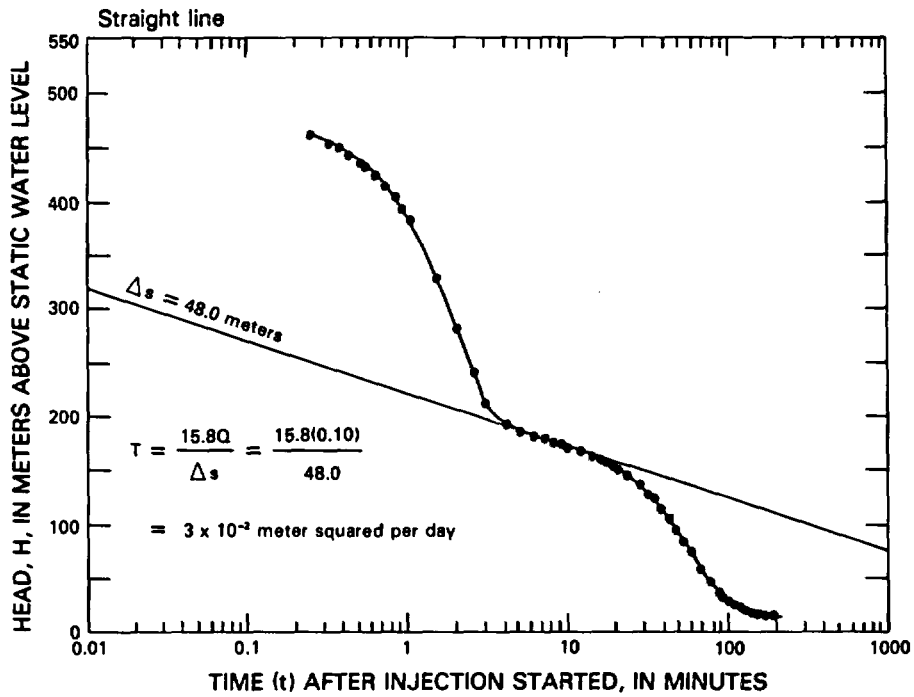


Figure 16.--Analysis of injection test of the interval from 972 to 1,219 meters, using straight-line and slug-test methods.

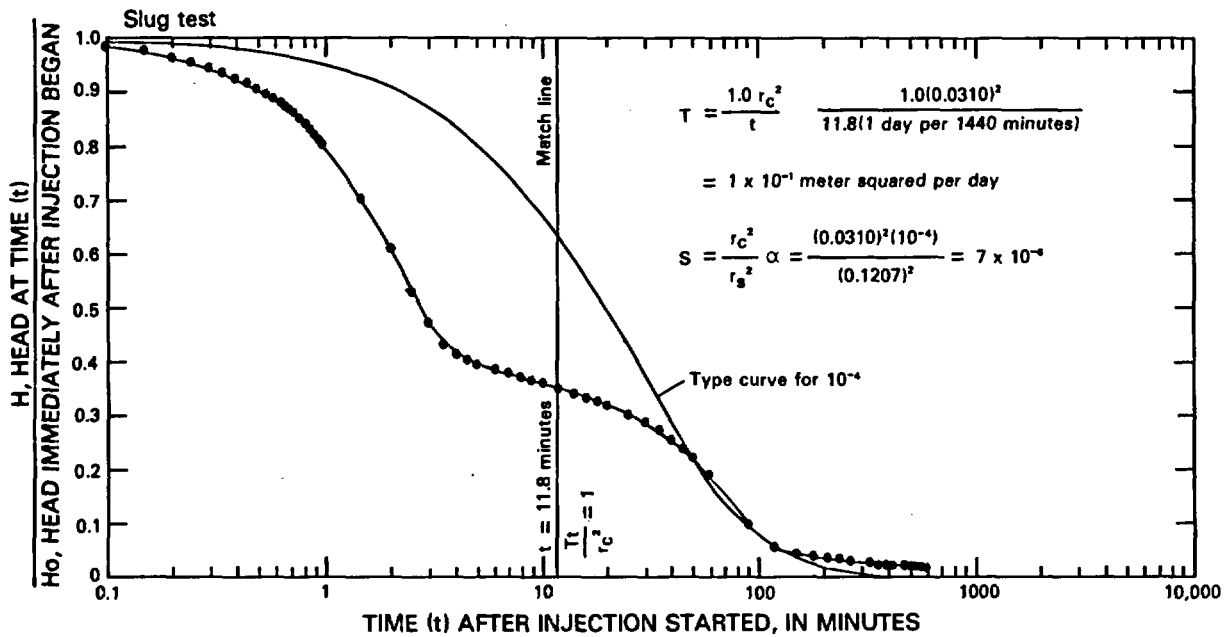
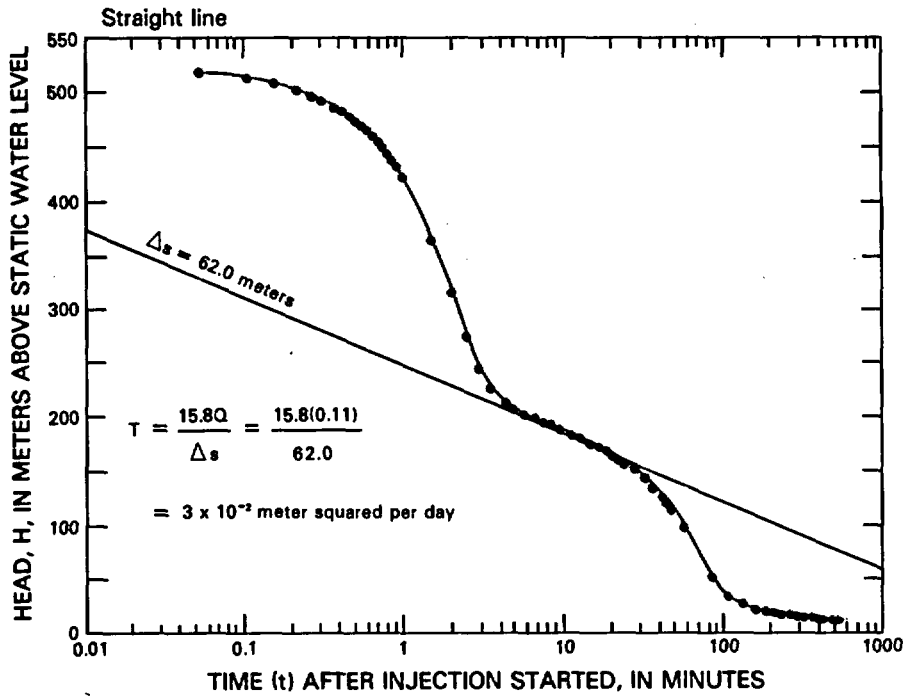


Figure 17.--Analysis of injection test of the interval from 1,063 to 1,124 meters, using straight-line and slug-test methods.

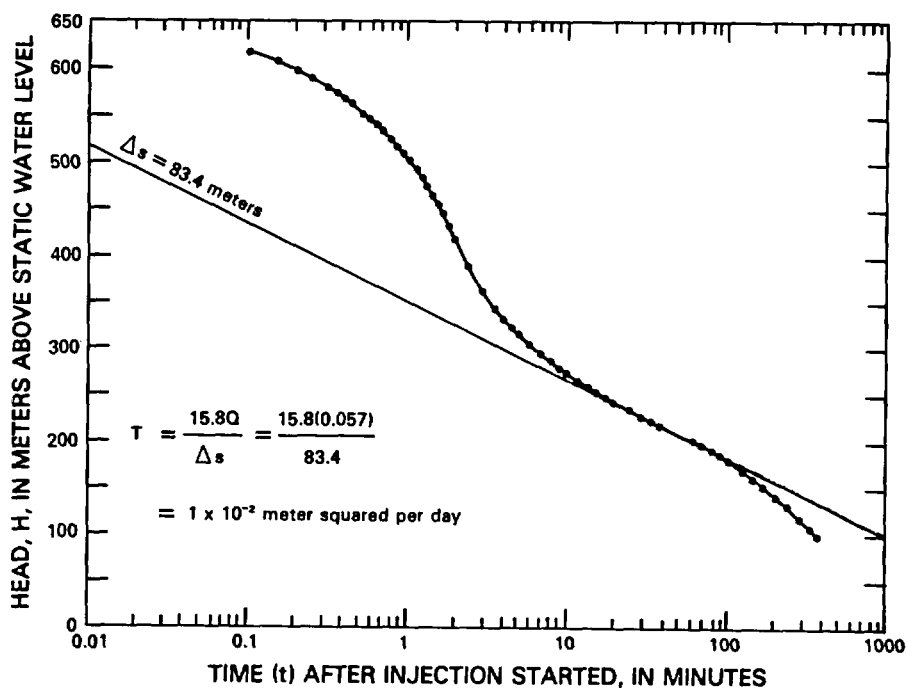


Figure 18.--Analysis of injection test of the interval from 1,126 to 1,219 meters, using the straight-line method.

In addition to the constraint on the use of early-time data for the injection tests, a second constraint needs to be considered for straight-line method of analysis of the test data. Constant rate of injection and values of  $\mu$  less than 0.01 are requirements to use the method of analysis correctly. The straight-line method was used on five of the six injection tests that show a straight line after about 8 minutes on the semilogarithmic plots. The injection rate of water was nearly constant during the middle part of the semilogarithmic straight line where this rate was within 2 to 22 percent of the average injection rate, as determined from the decline of water within the tubing. Therefore, the analysis was limited to the middle part of the data plots. The values of transmissivity range from  $1 \times 10^{-2}$  to  $1.2 \text{ m}^2/\text{d}$  using both the slug-test and straight-line methods (table 2).

The storage-coefficient values computed in figures 13, 15, 16, and 17 indicate that the tested zones were under artesian conditions. Based on estimates for storage coefficients by Lohman (1972, p. 8), the values listed in table 2 were very small, but probably were reasonable in magnitude. The values of storage coefficients range from  $4 \times 10^{-6}$  to  $7 \times 10^{-6}$  (table 2). For the injection tests, departure from ideal was variable; these departures are listed in table 2.

### Swabbing Tests

Swabbing tests consisted of multiple swabbing runs in the open uncased part of the well and between two inflatable straddle packers. Swabbing tests were analyzed using the straight-line method that was described previously in the section on pumping tests.

Analyses of the two swabbing tests are presented in figures 19 and 20. For the test interval from 792 to 1,219 m (fig. 19), the calculated value of transmissivity was 1.1 m<sup>2</sup>/d. The other test, for the interval from 1,063 to 1,124 m (fig. 20), had a calculated value of 1x10<sup>-1</sup> m<sup>2</sup>/d. Both sets of data had only small departures from ideal.

### Comparison of Testing and Borehole-Flow Survey Results

In the preceding sections of this report, values of transmissivity and storage coefficient were calculated from pumping, injection, and swabbing tests; results are summarized in table 2. In table 2, two values for transmissivity for the interval 792 to 1,219 m are listed: (1) Values from a swabbing test (fig. 19) of 1.1 m<sup>2</sup>/d, and (2) a value calculated from four injection tests spanning the surveyed interval (figs. 13-16), 1.4 m<sup>2</sup>/d. A slightly smaller interval, from 822 to 1,219 m, produced a slightly smaller value, 1.0 m<sup>2</sup>/d, from the long-term pumping test (fig. 6). The swabbing-test results appear to have the smaller departure of data from the ideal; as a result, the value from the swabbing test of 1.1 m<sup>2</sup>/d was selected as the more representative value for the interval (table 3).

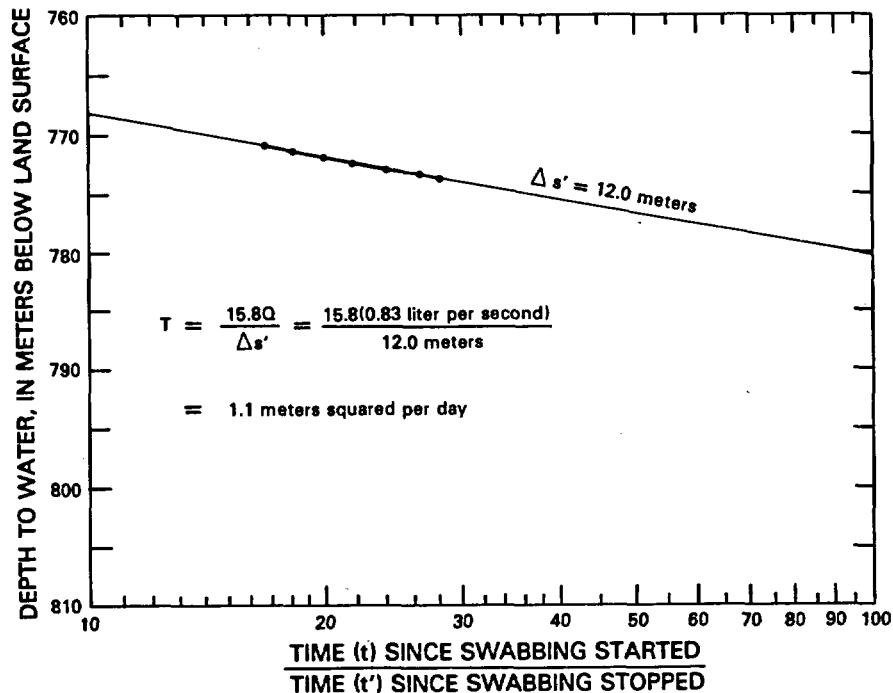


Figure 19.--Analysis of recovery of water level during swabbing test of the interval from 792 to 1,219 meters.

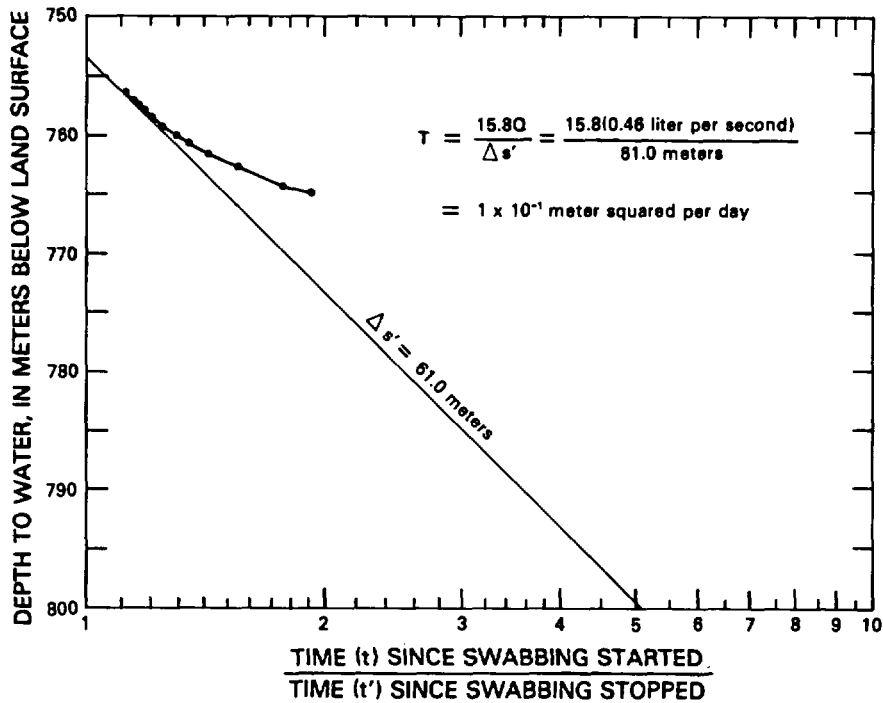


Figure 20.--Analysis of recovery of water level during swabbing test of the interval from 1,063 to 1,124 meters.

Based on the above-selected value of transmissivity for the interval 792 to 1,219 m and the borehole-flow survey for the same interval, apparent transmissivity was distributed throughout the interval in table 3. From the apparent transmissivity values, values for apparent average horizontal hydraulic conductivity were calculated.

Transmissivity values were calculated from pumping tests (table 2) for the test interval from 754 to 1,219 m, an interval that includes the smaller interval of the borehole-flow survey. The larger interval would be expected to have a similar or larger value for transmissivity, but smaller values were calculated ( $5 \times 10^{-1} \text{ m}^2/\text{d}$  and  $4 \times 10^{-1} \text{ m}^2/\text{d}$ ) in figures 4 and 5. The departure of data from ideal for these two tests seemed to be about the same as for the above-discussed swabbing test; therefore, the selected representative value of transmissivity for the penetrated part of the saturated zone, interval from 754 to 1,219 m, was computed as the average of the three values at about  $0.7 \pm 0.3 \text{ m}^2/\text{d}$ . Therefore, the values of transmissivity and hydraulic conductivity listed in table 3 should be considered maximum estimated values because they were based on a slightly higher transmissivity value.

An additional comparison of transmissivity values for a selected interval is presented in table 4. Although the three depth intervals are not identical, the overlap is about 95 percent. Conclusions drawn from the table are that the three tests produced similar results of the same order of magnitude and that the selected representative value for the interval from 1,063 to 1,124 m is about  $1 \times 10^{-1} \text{ m}^2/\text{d}$ .

Table 3.--Distribution of apparent transmissivity and hydraulic conductivity based on the borehole-flow survey

[Computations based on a transmissivity of 1.1 meters squared per day;  
<, less than]

Depth interval (meters)	Apparent transmissivity, T (meters squared per day)	Apparent average horizontal hydraulic conductivity, K (meters per day)
<u>TRAM MEMBER</u>		
1792 - 800	$<2 \times 10^{-2}$	$<3 \times 10^{-3}$
800 - 809	$<2 \times 10^{-2}$	$<2 \times 10^{-3}$
809 - 823	$3 \times 10^{-1}$	$2 \times 10^{-2}$
823 - 831.5	$3 \times 10^{-1}$	$3 \times 10^{-2}$
831.5- 832.1	$4 \times 10^{-2}$	$7 \times 10^{-2}$
832.1- 839	$<2 \times 10^{-2}$	$<3 \times 10^{-3}$
839 - 840.3	$<2 \times 10^{-2}$	$<2 \times 10^{-2}$
840.3- 840.9	$4 \times 10^{-2}$	$7 \times 10^{-2}$
840.9- 847	$<2 \times 10^{-2}$	$<3 \times 10^{-3}$
847 - 858	$2 \times 10^{-2}$	$2 \times 10^{-3}$
858 - 872	$<2 \times 10^{-2}$	$<1 \times 10^{-3}$
872 - 889	$<2 \times 10^{-2}$	$<1 \times 10^{-3}$
889 - 933	$5 \times 10^{-2}$	$1 \times 10^{-3}$
933 - 960	$<2 \times 10^{-2}$	$<7 \times 10^{-4}$
960 - 984	$<2 \times 10^{-2}$	$<8 \times 10^{-4}$
984 - 994	$<2 \times 10^{-2}$	$<2 \times 10^{-3}$
994 -1,009	$<2 \times 10^{-2}$	$<1 \times 10^{-3}$
1,009 -1,060	$<2 \times 10^{-2}$	$<4 \times 10^{-4}$
1,060 -1,083	$8 \times 10^{-2}$	$2 \times 10^{-3}$
<u>TRAM MEMBER AND BEDDED TUFF</u>		
1,083 -1,106.1	$2 \times 10^{-1}$	$7 \times 10^{-3}$
<u>BEDDED TUFF</u>		
1,106.1-1,108.3	$<2 \times 10^{-2}$	$<9 \times 10^{-3}$
<u>BEDDED TUFF AND LITHIC RIDGE TUFF</u>		
1,108.3-1,113.7	$4 \times 10^{-2}$	$7 \times 10^{-3}$

Table 3.--Distribution of apparent transmissivity and hydraulic conductivity based on the borehole-flow survey--Continued

Depth interval (meters)	Apparent transmissivity, T (meters squared per day)	Apparent average horizontal hydraulic conductivity, K (meters per day)
<u>LITHIC RIDGE TUFF</u>		
1,113.7-1,116.2	<2x10 <sup>-2</sup>	<8x10 <sup>-3</sup>
1,116.2-1,120.1	<2x10 <sup>-2</sup>	<5x10 <sup>-3</sup>
1,120.1-1,120.4	7x10 <sup>-2</sup>	2x10 <sup>-1</sup>
1,120.4-1,197.9	<2x10 <sup>-2</sup>	<3x10 <sup>-4</sup>
1,197.9-1,200.9	<2x10 <sup>-2</sup>	<7x10 <sup>-3</sup>
1,200.9-1,219	<2x10 <sup>-2</sup>	<1x10 <sup>-3</sup>

<sup>1</sup>Well cased to 792 meters.

Table 4.--Comparison of transmissivity values resulting from three types of tests

[<, less than]

Depth interval (meters)	Transmissivity (meters squared per day)	Type of test	Remarks
1,063-1,124	1x10 <sup>-1</sup>	Injection	Using value for interval from table 2 with least departure from ideal.
1,063-1,124	1x10 <sup>-1</sup>	Swabbing	From table 2.
1,060-1,120.4	<4x10 <sup>-1</sup>	Borehole- flow survey	Sum of values for seven intervals, table 3.

Values of transmissivity and hydraulic conductivity determined from the tests are very small, but are several orders of magnitude larger than those determined from tests of test well USW H-1 (Rush and others, 1984, table 14). To illustrate the low magnitude of the values, using a method by Theis (1963), if the well were pumped at a constant rate for 24 hours and the resulting drawdown were 100 m, the required well yield would be less than 1 L/s.

## DISCUSSION OF WELL-SITE GEOHYDROLOGY

In the previous sections of this report, results of the analyses of various sets of data are presented. In this section, all results are considered and data conflicts are resolved to develop a composite geohydrologic interpretation of each stratigraphic unit in the saturated-zone conceptual model and the units in the overlying unsaturated zone.

The Tiva Canyon Member crops out at the well site and has a thickness of 120 m (table 1). It is a densely welded to nonwelded ash-flow tuff with a thin bedded tuff at the base. The unit probably is fractured, with fractures extending from a depth of 9 m to 101 m. The unit probably is able readily to absorb percolating water from infiltration of infrequent runoff in the area. Runoff is from infrequent, localized, but commonly intense thundershowers during the spring and summer, and occasionally is from rapid snowmelt. The small quantity of water that is not returned to the atmosphere by evapotranspiration before it reaches a depth of about 15 m will continue percolating toward the regional water table, through this unit, and through several underlying units.

Underlying the Tiva Canyon Member and bedded tuff is the 301-m-thick Topopah Spring Member, a moderately to densely welded ash-flow tuff (table 1). The unit generally has abundance of rock that have less-than-average porosity. Fractures probably are common in the interval from 169 to 358 m. Slickensides were observed at a depth of 216 m, and a small water seep was identified at a depth of 277 m.

Tuffaceous beds of Calico Hills are a 29-m-thick unit of probably nonwelded ash-flow tuff (table 1). The unit has an abundance of rock having greater-than-average porosity. No fractures were observed with the down-hole television camera.

The Prow Pass Member is 126 m of nonwelded to partially welded ash-flow tuff overlying a thin-bedded tuff (table 1). Similar to the overlying unit, no fractures were observed by the television survey.

The Bullfrog Member is 165 m thick (table 1), at a depth of 581 to 746 m. It is an ash-flow tuff, mostly densely welded. Rock having greater-than-average porosity is not abundant in the member (fig. 2). During the drilling period, water was produced from the lower 2 m (744 to 746 m) of the unit; however, the water table was at 750.7 m in the underlying bedded tuff, from 746 to 755 m. Water in the Bullfrog Member may be perched above the bedded tuff, or it may only be water introduced during drilling.

The Tram Member is mostly a 341-m-thick, mostly partially welded, ash-flow tuff, underlain by a 13-m-thick bedded tuff (table 1). The entire unit and penetrated underlying units are saturated. Like the Bullfrog Member, the upper one-half of the unit does not have an abundance of rock having greater-than-average porosity; the lower one-half has more porous rock (fig. 2). Only minor fractures were observed, in the upper 13 m of the unit.

Two sets of linear features, probably fractures, were identified in the Tram Member from the acoustic-televiwer log. In the interval from 821 to 929 m, lineations dipping about 60° to 80° to the southwest were common. At a greater depth--the interval from 1,029 to 1,107 m--lineations dipping 70° to 85° to the northeast and east were logged. Because the principal conductive zone for the well is from 809 to 840.9 m (table 3), most of these probable fractures do not conduct significant amounts of ground water.

Beneath the Tram Member and the thin, underlying bedded tuff, the well penetrated 110 m of Lithic Ridge Tuff. It is a partially welded, relatively porous ash-flow tuff (table 1). A thin interval from 1,120.1 to 1,120.4 m was more conductive than the remainder of the unit (table 3).

All the saturated rocks have very small apparent, average horizontal hydraulic conductivity (table 3). The order of magnitude of hydraulic conductivity generally ranges from  $10^{-2}$  to  $10^{-4}$  m/d. The calculated values of storage coefficient are very small also, ranging from  $4 \times 10^{-6}$  to  $7 \times 10^{-6}$  for four tests (table 2). Transmissivity of the penetrated part of the saturated zone, mostly rocks of the Tram Member, is no greater than about 1 m<sup>2</sup>/d.

#### CONCLUSIONS

At the site of this well, results of hydraulic tests, hydrologic monitoring, and geophysical log interpretations indicate that:

1. The Bullfrog Member and the overlying stratigraphic units commonly have intervals that are intensively fractured and relatively porous. They generally are unsaturated and are permeable to downward percolating water recharging the ground-water system from precipitation and runoff. However, the quantity of recharge from precipitation and runoff is very small because of the water-availability limits imposed by the desert climate.

2. The water table is at a depth of 750.7 m in the bedded tuff underlying the Bullfrog Member. In the 2-m-thick interval at the base of the Bullfrog Member, perched water or drilling fluids may be present. All saturated strata to the total depth of the well have very small permeability.

3. The most transmissive part of the saturated zone is in the upper part of the Tram Member, the interval from 809 to 840.9 m. The penetrated part of the saturated zone has an apparent horizontal transmissivity of about 1 m<sup>2</sup>/d or less.

4. The conceptual model presented in this report is a reasonable representation of the actual fracture-flow system near the test well.

## REFERENCES CITED

- Baecher, G. B., 1983, Statistical analysis of rock mass fracturing: *Mathematical Geology*, v. 15, no. 2, p. 329-348.
- Birdwell Division, 1973, Geophysical well log interpretation: Tulsa, Seismograph Service Corporation, 188 p.
- Blankennagel, R. K., 1967, Hydraulic testing techniques of deep drill holes at Pahute Mesa, Nevada Test Site: U.S. Geological Survey Open-File Report, 50 p.
- \_\_\_\_\_, 1968, Geophysical logging and hydraulic testing, Pahute Mesa, Nevada Test Site: *Ground Water*, v. 6, no. 4, p. 24-31.
- Blankennagel, R. K., and Weir, J. E., Jr., 1973, Geohydrology of the eastern part of Pahute Mesa, Nevada Test Site, Nye County, Nevada: U.S. Geological Survey Professional Paper 712-B, 35 p.
- Bredehoeft, J. D., and Maini, Tidu, 1981, Strategy for radioactive waste disposal in crystalline rocks: *Science*, v. 213, no. 4505, p. 293-296.
- Byers, R. M., Jr., Carr, W. J., Orkild, P. P., Quinlivan, W. D., and Sargent, K. A., 1976, Volcanic suites and related calderas of Timber Mountain-Oasis Valley caldera complex, southern Nevada: U.S. Geological Survey Professional Paper 919, 70 p.
- Cooper, H. H., Jr., Bredehoeft, J. D., and Papadopoulos, S. S., 1967, Response of a finite-diameter well to an instantaneous charge of water: *Water Resources Research*, v. 3, no. 1, p. 263-269.
- Cooper, H. H., Jr., and Jacob, C. E., 1946, A generalized graphical method for evaluating formation constants and summarizing well-field history: *American Geophysical Union Transactions*, v. 27, no. 4, p. 526-534.
- Earlougher, R. C., 1977, Advances in well test analysis: Dallas, Society of Petroleum Engineers of America Institute of Mining, Metallurgical, and Petroleum Engineers, Inc., 264 p.
- Ferris, J. G., Knowles, D. B., Brown, R. H., and Stallman, R. W., 1962, Theory of aquifer tests: U.S. Geological Survey Water-Supply Paper 1536-E, 174 p.
- Freeze, R. A., and Cherry, J. A., 1979, *Groundwater*: Englewood Cliffs, New Jersey, Prentice-Hall, Inc., 604 p.
- Hubbert, M. K., and Willis, D. G., 1972, Mechanics of hydraulic fracturing, in Cook, T. D., ed., *Underground waste management and environmental implications*: Tulsa, Oklahoma, American Association of Petroleum Geologists Memoir 18, p. 238-257.
- Hunt, C. B., Robinson, T. W., Bowles, W. A., and Washburn, A. L., 1966, Hydrologic basin, Death Valley, California: U.S. Geological Survey Professional Paper 494-B, 138 p.
- Kazemi, Hossein, 1969, Pressure transient analysis of naturally fractured reservoirs with uniform distribution: *Society of Petroleum Engineers Journal*, v. 9, no. 4, p. 451-462.
- Kazemi, Hossein, and Seth, M. S., 1969, The interpretation of interference tests in naturally fractured reservoirs with uniform fracture distribution: *Society of Petroleum Engineers Journal*, v. 9, no. 4, p. 463-472.
- Lohman, S. W., 1972, *Ground-water hydraulics*: U.S. Geological Survey Professional Paper 708, 70 p.
- Najurieta, H. L., 1980, A theory for pressure transient analysis in naturally fractured reservoirs: *Journal of Petroleum Technology*, July, p. 1241-1250.

- Odeh, A. S., 1965, Unsteady-state behavior of naturally fractured reservoirs: Society of Petroleum Engineers Journal, v. 5, no. 1, p. 60-65.
- Papadopoulos, S. S., Bredehoeft, J. D., and Cooper, H. H., Jr., 1973, On the analysis of "slug test" data: Water Resources Research, v. 9, no. 4, p. 1087-1089.
- Rush, F. E., 1970, Regional ground-water systems in the Nevada Test Site area, Nye County, Lincoln, and Clark Counties, Nevada: Nevada Department of Conservation and Natural Resources, Division of Water Resources, Water Resources Reconnaissance Series Report 54, 25 p.
- Rush, F. E., Thordarson, William, and Pyles, D. G., 1984, Geohydrology of test well USW H-1, Yucca Mountain, Nye County, Nevada: U.S. Geological Survey Water-Resources Investigations Report 84-4032, 56 p.
- Sass, J. H., and Lachenbruch, A. H., 1982, Preliminary interpretation of thermal data from the Nevada Test Site: U.S. Geological Survey Open-File Report 82-973, 30 p.
- Schlumberger Limited, 1972, Log interpretation, volume 1--Principles: New York, 113 p.
- Scott, R. B., Spengler, R. W., Diehl, Sharon, Lappin, A. R., and Chornack, M. P., 1983, Geologic character of tuffs in the unsaturated zone at Yucca Mountain, southern Nevada, in Role of the unsaturated zone in radioactive and hazardous waste disposal, Ann Arbor Science Publishers, Ann Arbor, Michigan, p. 289-335.
- Theis, C. V., 1963, Chart for the computation of drawdown in the vicinity of a discharging well, in Bentall, Ray, compiler, Shortcuts and special problems in aquifer tests: U.S. Geological Survey Water-Supply Paper 1545-C, p. C10-C15.
- Thordarson, William, Rush, F. E., Spengler, R. W., and Waddell, S. J., 1984, Geohydrologic and drill-hole data for test well USW H-3, adjacent to Nevada Test Site, Nye County, Nevada: U.S. Geological Survey Open-File Report 84-149, 28 p.
- Waller, R. M., Turk, J. T., and Dingman, R. J., 1978, Potential effects of deep-well waste disposal in western New York: U.S. Geological Survey Professional Paper 1053, 39 p.
- Wang, J. S. Y., Narasimhan, T. N., Tsang, C. F., and Witherspoon, P. A., 1977, Transient flow in tight fractures, in Division of Geothermal Energy, U.S. Department of Energy and Earth Science Division, Lawrence Berkeley Laboratory, Invitational well-testing symposium proceedings: October 19-21, 1977, 103-116.
- Warren, J. E., and Root, P. J., 1963, The behavior of naturally fractured reservoirs: Society of Petroleum Engineers Journal, v. 3, no. 3, p. 245-255.
- Winograd, I. J., and Thordarson, William, 1975, Hydrologic and hydrochemical framework, south-central Great Basin, Nevada-California, with a special reference to the Nevada Test Site: U.S. Geological Survey Professional Paper 712-C, 126 p.
- Witherspoon, P. A., Cook, N. G. W., and Gale, J. E., 1980, Progress with field investigations and Stripa: University of California, Lawrence Berkeley Laboratory, Earth Science Division Technical Information Report No. 27, 50 p.

